

Thesis.  
1961(F)  
# 43

THE UNIVERSITY OF ALBERTA

"VARIATIONS IN EXTENSIVE AIR SHOWERS"

A THESIS

SUBMITTED TO THE FACULTY OF GRADUATE STUDIES  
IN PARTIAL FULFILMENT OF THE REQUIREMENTS FOR THE DEGREE  
OF MASTER OF SCIENCE

DEPARTMENT OF PHYSICS

BY

DEREK B. SWINSON

CALGARY, ALBERTA

SEPTEMBER, 1961

© Derek B. Swinson 1971

— ABSTRACT —

A horizontal array of 18 Geiger-Mueller counters has been used to detect extensive air showers over a period of two years at Sulphur Mountain observatory, 2283 m altitude, and at Calgary, 1086 m altitude, for a period of 200 days. Analysis of data leads to the conclusion that at Sulphur Mountain, E.A.S. are isotropic in solar time to within 1.45 % and in sidereal time to within 1.07 %; in Calgary E.A.S. are isotropic in sidereal time to within 4.6 %. A value of  $\gamma$ , the exponent of the density spectrum, of  $1.5 \pm 0.1$  was obtained for showers up to a density of 500 particles / m<sup>2</sup>, and was found to increase above this density to a value of 1.9 for densities  $10^3 - 10^4$  particles / m<sup>2</sup>. A barometer coefficient of 16.46 % / cm. Hg was found for E.A.S. of energy from  $10^{14}$  to  $10^{16}$  e.v., and for E.A.S. of  $10^{14} - 10^{15}$  e.v. a temperature coefficient of - 0.34 % / °C was obtained.

### ACKNOWLEDGEMENTS

The author would like to thank Dr. B. G. Wilson of the University of Alberta, Calgary, who planned and supervised the experiment.

Thanks are due to the University of Alberta, for a teaching assistantship for the year 1960 - 61, and also for taking care of travelling expenses for frequent trips between the University in Calgary and the Laboratory in Banff.

The author is grateful to Mr. D. Will and Mr. C. Hansen for their help in maintaining the apparatus, and to Mrs. T. Will and Mrs. F. Gulleksen for their help in the analysis of the data.

<u>Table of Contents</u>	<u>Page</u>
List of Tables	vi
List of Figures	vii
Introduction	1
Time Variations in Extensive Air Showers	4
Experimental Apparatus	20
Calculation of the energy of E.A.S. detected by the Banff apparatus	22
Analysis of Data	35
(a) Time Variations	35
(b) Density Spectrum	38
(c) Barometer Coefficient	40
(d) Temperature Coefficient	42
Conclusion	60
(a) Time Variations	60
(b) Density Spectrum	62
(c) Barometer Coefficient	62
(d) Temperature Coefficient	63
Bibliography	64
General References	65

List of TablesPage

<u>No.</u>	<u>Title</u>	
1	Results of time variation experiments on E.A.S. in Sidereal time (Reproduced from Galbraith)	6
2	Results of time variation experiments on E.A.S. in Solar time (Reproduced from Galbraith)	17
3	Particle density $\rho(N,r)$ , for different values of $r$ and $N$ , in particles / $m^2$	24
4	Area capable of producing 3-6, 7-12 and 13-18 fields for different values of $N$ .	24
5	Frequency x Area for 3-6, 7-12 and 13-18 fields with $\gamma = 1.5$	28
6	Frequency x Area for 3-6, 7-12 and 13-18 fields with $\gamma = 1.9$	28
7	Probabilities of data representing a straight line or a sine wave for the various components	39
8	Experimental number of showers and expected number of showers assuming a variable $\gamma$ .	41

# List of Figures

<u>No.</u>	<u>Title</u>	<u>Page</u>
1	(a) Arrangement of G.M.C. containers in the laboratory	
	(b) Arrangement of G.M.C. in containers	18
2	Block diagram of apparatus	19
3	(a) Distance R from axis VS particle density for $N = 10^5$	25
	(b) Distance R from axis VS particle density for $N = 10^6$	26
	(c) Distance R from axis VS particle density for $N = 10^7$	27
4	Frequency VS number of particles for $\gamma = 1.9, 1.5$	32
5	Probability P VS number of particles for 3-6, 7-12, and 13-18 fields with $\gamma = 1.5$ .	33
6	Probability P VS number of particles for 3-7, 7-12 and 13-18 fields with $\gamma = 1.9$ .	34
7	Sheet for recording data	36
8	Banff 3-6 field sidereal (a) hourly	
	(b) 3-hourly	43
9	Banff 7-12 field sidereal (a) hourly	
	(b) 3-hourly	44
10	Banff 13-18 field sidereal (a) hourly	
	(b) 3-hourly	45
11	Banff total sidereal (a) hourly	
	(b) 3-hourly	46
12	Calgary 3-6 field sidereal (a) hourly	
	(b) 3-hourly	47

<u>No.</u>	<u>Title</u>	<u>Page</u>
13	Calgary 7-12 feld sidereal (a) hourly	
	(b) 3-hourly	48
14	Calgary 13-18 feld sidereal (a) hourly	
	(b) 3-hourly	49
15	Calgary total sidereal (a) hourly	
	(b) 3-hourly	50
16	Banff 3-6 feld solar (a) hourly	
	(b) 3-hourly	51
17	Banff 7-12 feld solar (a) hourly	
	(b) 3-hourly	52
18	Banff 13-18 feld solar (a) hourly	
	(b) 3-hourly	53
19	Banff total solar (a) hourly	
	(b) 3-hourly	54
20	Experimental number of showers VS multiplicity compared with predicted values with $\delta = 1.4, 1.5$ and $1.6$ .	55
21	Experimental number of showers VS multiplicity compared with predicted values using a variable $\delta$ .	56
22	E.A.S. rate in counts per hour VS daily average pressure.	57
23	(a) Banff monthly mean temperature VS month of year.	
	(b) 3-6 feld monthly mean rate VS month.	
	(c) 7-12 feld monthly mean rate VS month.	58
24	(a) Banff monthly mean temperature VS month of year	
	(b) 13-18 feld monthly mean rate VS month	
	(c) Total monthly mean rate VS month.	59

## Introduction

When a high energy primary cosmic ray particle interacts high in the atmosphere with an oxygen or nitrogen nucleus, it produces a shower of particles, forming a cone of very narrow angle, which eventually causes a large number of particles to arrive at the earth within a few micro-seconds of each other; such an event is known as an "extensive air shower." (E.A.S.).

Much of the early work on E.A.S. was done by the Auger group working in Paris; they found coincidences between counters separated by distances of up to 300 m. E.A.S. were observed by Janssny and Levell in 1938 using a cloud chamber containing a lead plate, in which the multiplication of particles established their predominantly electronic nature. Slow proton tracks were found in the showers by the Auger group inferring the presence of a nuclear active component consisting of protons and neutrons. In 1939 the Auger group measured transition effects and absorption curves demonstrating the predominant abundance of electrons and photons in E.A.S. as well as the presence of a small penetrating component capable of penetrating more than 20 cms. of lead.

Because of the large number of particles, it was clear that E.A.S. represented the effects of primary cosmic rays of extremely high energy. This fact accounts for the two principal reasons for the study of E.A.S. :- to obtain information relating to the origin of the primary cosmic radiation, and to investigate the nature of the interactions of very high energy particles; particles of such high energies cannot be produced by present accelerators, and it seems unlikely that energies of



$10^{18} - 10^{19}$  e.v. could be produced in this way.

For several years it was thought that the E.A.S. represented the effects of primary electrons or  $\gamma$ -rays of very high energy. The small number of mesons and nucleons were thought to be secondary to the more numerous photons and electrons. Later, however, both theory and experiments have indicated that there are practically no electrons or photons in the primary radiation, though very recently Earl found<sup>1</sup> that 3 % of the primary particles were electrons. It has become evident that the photons and electrons are themselves the secondary component, while the E.A.S. are initiated and dominated in their development by the nuclear active particles. The primary effect is a nucleon cascade i.e. a series of high energy nuclear collisions occurring at various depths in the atmosphere. An incoming primary particle collides high in the atmosphere with an oxygen or nitrogen nucleus, giving rise to a shower of mesons and nucleons which continue towards the earth approximately along the projected axis of the incoming particle; this central region around the axis is called the "core" of the shower. Further nuclear disintegrations are produced by these axial particles, giving rise to more mesons, hyperons, nucleons and anti-nucleons constituting the nucleon cascade. Decay of secondary K mesons and charged  $\pi$  mesons give rise to the  $\mu$ -component which does not multiply further and is slowly absorbed by ionisation and  $\beta$ -decay. Decay of  $\pi^0$ 's throughout the cascade transfers energy to photons, each of which initiates an e.m. cascade by forming a positron and an electron forming further photons by the "Bremsstrahlung" process. These e.m. cascades rapidly grow to comprise the most numerous particles in the shower.

Individual e.m. cascades have a small range compared with the thickness of the atmosphere, but are continuously regenerated by the nuclear cascade, so that the soft component gradually dies out as a source of energy as the N -component becomes depleted. Ultimately the most numerous particles remaining are the  $\mu$  - mesons.

Composition of a single air shower and the energy spectra of the components undergo major changes as the shower develops and decays. The nuclear cascade is the core of the shower; the number of nucleus-nucleus interaction lengths in the vertical atmosphere is only 13, hence fluctuations in the height of the first interaction, and in the rate of shower growth, are very large, and showers of a given energy are encountered at a single altitude at all stages of development. The least possible energy for a shower of given size is the energy for which that shower would be at its maximum development. Any shower that is very far from this condition will be rare among other showers of the same size due to the steepness of the energy spectrum, therefore the majority of showers recorded at almost any elevation are in nearly the same stage of development.

### Time Variations in Extensive Air Showers

One of the main reasons for studying E.A.S. is to gain information on the origin of the primary particles of cosmic radiation. This is best studied by monitoring showers over a long period and analysing the results in solar and sidereal time to see if there is a preferential arrival direction.

A time variation in the arrival of E.A.S. may be due to the combination of two effects: - (1) variations in the intensity of the incoming primary radiation (2) variations in the secondary component due to changes in the atmospheric density caused by pressure or temperature changes. Time variations are generally looked for in solar time and in sidereal time, that is time with respect to the first point in the constellation Aries; the sidereal day is four minutes shorter than the solar day due to there being 366 sidereal days in one solar year. There is no reason to expect a primary variation in solar time for E.A.S. since it is unlikely that the sun would emit such high energy particles. A sidereal time variation would give some evidence for the origin of cosmic radiation since, due to the high energies of the particles causing the showers, it would seem that these primaries are of galactic or extra-galactic origin and a maximum in sidereal time would indicate what part of the galaxy was overhead at that time.

One way to detect time variations is to note the counting rate of a given arrangement of apparatus as a function of solar and sidereal time, using the rotation of the earth to direct the apparatus at different parts of the sky.

### Sidereal Variations.

Sidereal time variations in E.A.S. may be because of an asymmetry in the directional distribution of high energy primary cosmic rays outside the earth. The different possible causes of such an asymmetry would presumably be indicated by the presence or absence of such effects in the experimental observations and we may thus get information about the origin and acceleration of cosmic rays, and about the nature of space through which they travel before reaching the earth. If, for instance, interstellar space were field-free, the cosmic rays would travel in straight lines from their sources; non-uniform distribution of likely stellar sources would therefore cause some anisotropy. It is unlikely, however, that there are no fields in inter-stellar space since the energy density of cosmic rays is difficult to explain without the aid of some storage mechanism and also because the primary cosmic rays appear to be extremely isotropic; the amplitudes found of the variations of intensity with sidereal time are extremely small (See Table I).

Bierman and others<sup>2</sup> conclude that fields of the order of  $10^{-6}$  to  $10^{-5}$  gauss would have arisen out of the turbulent motions of ionised gases in the galaxy, even if there had been no field in the beginning. The magnetic fields provide a convenient means of storing cosmic-ray energy in the galaxy, and of randomising the directional intensity.

According to Fermi's theory of the acceleration of Cosmic rays, the fields are considered to be oriented at random, stirred up, and carried

Experiment	Altitude	Total Counts N	Primary Energy e.v.	Amplitude per cent	Time of Max. G.M.P.	P % *
Daudin et al.	2860 m		$3 \cdot 10^{14}$	0.09	2030	
			$2 \cdot 10^{15}$	0.17	2130	
Citron	1200 m		$10^{15}$	0		
Hodson	Near S.L.		$5 \cdot 10^{14}$	1.15	2330	
Farley & Storey	Near S.L.	$3 \cdot 10^5$		1.43	1730	
Cranshaw		3414	$2 \cdot 10^{16}$	1.7		70
and Elliot	Near S.L.	711	$10^{17}$	7.5		20
Cranshaw and	Near S.L.	71000	$10^{16}$	0.6	1320	49
Galbraith - I		22000	$2 \cdot 10^{16}$	2.0	0930	10
		8500	$5 \cdot 10^{16}$	4.9	1100	1
		500	$10^{17}$	10.1	0400	27
Cranshaw and	Near S.L.	37000	$7 \cdot 10^{16}$	0.14		84
Galbraith - II		7200	10	2.0		51
		1900	$2 \cdot 10^{17}$	0.2		99
		150	$10^{18}$	8.3		76

Table 1. Results of Time Variation Experiments in Sidereal Time.

(Reproduced from Galbraith).

\* P is the probability that the observed amplitude could arise as a result of statistical fluctuations in the sample of N counts.

about by the turbulent motion of clouds of ionised gas. It is assumed that the cosmic rays leak out of the galaxy in an average time of  $10^6$  years to account for the charge spectrum of the primaries. To account for the energy spectrum and the nearly perfect isotropy of the cosmic rays, the clouds must be assumed to have both a high R.M.S. velocity (120 Km/sec) and a small size. As long as the mean scattering length is independent of the energy the anisotropy remains small and independent of energy. At energies so high that the particles can penetrate through the magnetic clouds, the isotropy must cease, the acceleration mechanism must fail, and there is a large escape probability, implying a cut-off in the intensity.

There has not however been any evidence of a cut-off in the high energy particle spectrum, and the existence of particles up to  $10^{19}$  e.v. has been shown.<sup>3</sup> According to the above theory, however, protons of  $2 \cdot 10^{17}$  e.v. moving normal to a magnetic field of  $10^{-6}$  gauss would have a radius of curvature of 700 light years, about equal to the thickness of the galactic disc. This would suggest that the spectrum would become appreciably steeper at an energy of about  $10^{15}$  e.v. with a "cut-off energy" of approximately  $10^{17}$  e.v. Also the high velocity required of the clouds is hard to reconcile with direct observations.

The plane of polarisation of starlight however suggests the fields are not random, but are coherently oriented, apparently along the arms of the galaxy. If the turbulent elements of the magnetic fields are dominated by a coherent field having an extension as wide as the galactic arms, there is no difficulty in accounting for the retention within the galaxy of cosmic rays of energy up to  $10^{18}$  e.v. Considering the concept of superposition of magneto-hydrodynamic waves on a nearly uniform field,

directed along the galactic arms, Davis<sup>4</sup> pictures the cosmic rays as spiraling along the lines of force in the magnetic field, frequently reversing the component of motion along the field by colliding with a shock front where the field intensity changes rapidly. Very high energies are attained over a long period of time, by a statistical accumulation of small accelerations owing to betatron action and to reflections from the moving shock fronts; consequently the arrival direction of high energy cosmic rays at earth bears no relation to the direction from the original source, therefore any anisotropy would not be related to the distribution of sources, but to the properties of the magnetic field and the process of acceleration.

One of the causes of asymmetry is a net diffusion of the Cosmic rays along the field lines towards the nearest point of escape from the galaxy, and a minimum in the reverse direction. Davis has estimated the time of the maximum to be 20h L.S.T. There may also be asymmetry which is proportional to the gradient of the cosmic ray density normal to the magnetic field, and to the radius of curvature of the trajectories. This effect would increase strongly with the primary energy, and like the asymmetry due to diffusion, it would give rise to a 24 - hour period in the observed intensity, but with a different phase.

Further asymmetry may be due to the mechanism of acceleration, and will be significant if the acceleration of cosmic rays by interaction with the magnetic fields is responsible for an important part of the Cosmic ray energy. Davis has shown that the asymmetry arising from the acceleration process should show the existence of a second harmonic, and that the first harmonic should have its maximum 12 hours later for the Southern hemisphere than in the Northern hemisphere.

One might hope to learn from experiments whether or not the qualitative descriptions of the asymmetry fit the facts and which of the causes of asymmetry is predominant. At present a more generally held theory for the origin and acceleration of Cosmic rays is that of Ginzburg<sup>5</sup> who suggests that all existing information leads naturally to the hypothesis that cosmic radiation originates in the expanding envelopes of supernovae and possibly novae. Coming out into the interstellar medium from the envelopes of these stars, which lie in the region of the galactic plane, Cosmic ray particles fill the whole galaxy and there lose their energy mainly as a result of nuclear collisions.

Considering all the stars in our galactic system emitting at the same rate as our sun, they would only produce cosmic ray energy  $10^{32} - 10^{33}$  ergs/sec which is six to eight orders of magnitude short of the observed value of  $10^{39} - 10^{40}$  ergs/sec; supernovae and novae, however satisfy the energy requirements. It appears that the envelopes of nearly all known supernovae are powerful sources of radio emission which establishes the presence of relativistic electrons in these envelopes. After about 1,000 to 3,000 years the envelopes of the supernovae are dispersed into the interstellar medium; this also happens to the cosmic ray particles enclosed in the envelopes. Thus supernovae and novae can inject into the galaxy cosmic ray electrons at a power adequate to maintain an energy balance in the galaxy. If we consider the mechanism of the acceleration of particles in the envelopes of supernovae it becomes clear that the transfer of energy to protons and nuclei in quantities ten to a thousand times that going to the electrons is possible and probable. The particles undergo



statistical acceleration, and also acceleration of particles to relativistic energies may take place in the explosion process at the central star before the envelope has separated from it; further acceleration may arise from inductive acceleration connected with probable increase of magnetic field.

Under statistical acceleration the energy reached by a particle is proportional to its mass, therefore protons will be accelerated to an energy  $M/m$  times greater than electrons, and heavier nuclei to even greater energies. The observed spectrum of E.A.S. extends up to  $10^{19}$  e.v.; such energies can still be reconciled with the theory of galactic origin of Cosmic rays, provided the particles with the greatest energies are heavy nuclei, and there is a considerable excess of heavy nuclei over the natural abundance, observed in Cosmic rays. If however it is the primary protons that have energy up to  $10^{19}$  e.v. one can apparently conclude that the ultra high energy particles are of extra-galactic nature.

Ginzburg suggests that a reflection of particles at the spherical boundary of the galaxy leads to an averaging of the concentration and to a reduction of asymmetry. Because of the decrease of the coefficient of diffusion near the galactic plane, diffusion will occur mainly in the region of the galactic corona, and at the solar system the main diffusion inwards would not come from the galactic centre, but from above and below (i.e. from the directions normal to the galactic disc). This fact would tend to reduce any asymmetry.

## Experimental Results.

In 1951 Hodson found a sidereal diurnal variation with an amplitude of  $1.15 \pm .61\%$  with a maximum at 23.30 L.S.T.

In 1952 Daudin at 2860 m on the Pic du Midi reported a sidereal variation with an amplitude of  $0.39 \pm .13\%$  with a maximum at 22.00 L.S.T.

Farley and Sterey suggest that any such effect is less in the Northern hemisphere than in the Southern hemisphere because of the narrow polar diagram for reception, if particles come from the galactic centre. In an experiment in Auckland, New Zealand, Farley and Sterey studied E.A.S. of  $3.10^5$  particles at a height of 40 m, from February 1951 - February 1952. They selected electrons of median energy 100 Mev coming in vertically to within  $\pm 7$  degrees. Results for solar time indicated a clearly visible solar diurnal variation, apparently correlated with ground temperature, of amplitude  $1.45 \pm 0.25\%$  with a maximum at  $2.7 \pm .06$  hours solar time; the apparent temperature coefficient was  $-0.51\% / ^\circ\text{C}$ . There was also a significant 24 hour sidereal variation, which, by least squares analysis, had an amplitude of  $1.1 \pm .26\%$  at  $19.8 \pm .9$  hours L.S.T.

If the observed sidereal variations are due solely to seasonal modulation of solar diurnal variation (assumed the same in both hemispheres) we would expect the apparent sidereal variation to differ by 180 degrees in phase in the two hemispheres. In fact variations at the following three stations are in phase and maxima coincide in L.S.T. almost to within the probable error: -

Manchester	53	N		$23.5 \pm 2.0$	L.S.T.
Pic du Midi	43	N	Have maxima at	$22.0 \pm 1.3$	L.S.T.
Auckland	37	S		$19.8 \pm .9$	L.S.T.

All correspond to when the Milky Way is overhead; this occurs at 22.0 hours at the Pic du Midi and 17.7 hours at Auckland. This suggests cosmic rays come preferentially from regions of high star density in the galactic plane. Evidence suggests the amplitude is larger in the S. hemisphere and therefore it would appear that the direction from which the maximum cosmic ray intensity comes is in the galactic plane.

Cranshaw and Galbraith, 1954, using sixteen Geiger tubes each 200 cm<sup>2</sup> sensitive area, in a square lattice 4 x 4 with 54 m between counters, counted showers of energy  $10^{16}$ ,  $2 \cdot 10^{16}$ ,  $5 \cdot 10^{16}$  and  $10^{17}$  e.v. for coincidences 3-fold up to 8-fold. In sidereal time they found no striking variation outside the statistical accuracy of their results. They found a similar isotropy in solar time.

Cranshaw and Galbraith in a search for variations of Cosmic ray intensity at high energies  $10^{16}$  -  $10^{17}$  e.v. used counter sets separated by 150 m and 300 m (the counters were at the corners of a quadrilateral 150 m X 300 m.) At 150 m separation, coincidences corresponded to a shower initiated by a primary of  $2 \cdot 10^{16}$  e.v. and for 300 m separation, a primary energy of  $10^{17}$  e.v. For solar time there was no significant variation for  $10^{16}$  e.v. showers. For  $10^{17}$  e.v. showers they found a solar variation, the amplitude of whose first harmonic was 19.3%. For sidereal time none of the calculated amplitudes were statistically significant. The authors stated that the reality of the 19.3% solar variation was in

doubt.

In an attempt to locate a point source for cosmic radiation, Sekide in Japan studied the diurnal variation of very high energy cosmic rays underground. No solar variation was obtained, but there was a sidereal time variation with maximum at 05.20 L.S.T. Near the direction of the axis of the instrument at this time one can find the Crab nebula, a remarkable point source of cosmic noise. There was also a small peak at 20.00 L.S.T.

With regard to point sources Greisen suggests that if for example the Crab nebula has resulted in intense production of cosmic rays then, because of the intervening fields, these cosmic rays diffuse towards the earth with a mean scattering length of a few light years. The nebula is several thousand light years from the earth, hence although brilliant visible light began arriving here about 900 years ago, we should not expect the cosmic rays until millions of years have elapsed. No supernova visible in human history has had time to signal us with charged particles. Conversely, if a large influx of charged cosmic radiation is ever interpretable as an indication of unique sources, it will refer to activity in the distant past, and one should not expect to be able to see any longer a visible indication of the unusual activity, nor to detect it with radio waves.

In 1954 - 7 the Rossi<sup>3</sup> group at sea level, examined showers of from  $5 \cdot 10^5$  to over  $10^9$  particles. The core locations, arrival directions, and particle density distributions of several thousand showers whose cores landed within an area of  $10^5 \text{ m}^2$  were determined by the techniques of fast-timing and density sampling. They used large-area plastic scintillation

detectors, which could measure particle densities and arrival times, spread over an area of  $10^5 \text{ m}^2$ . The output of each channel was displayed on a separate cathode ray tube for measurement of relative arrival times. These data, together with the time of day, the day of year, calibration data and various instrumental and astronomical constants were processed by computer to give the zenith angle, right ascension and declination of the source of the shower. They estimated their errors as less than 5% in arrival direction. They plotted the distributions of arrival directions for showers of average size  $1.8 \times 10^7$  particles and for N greater than  $10^8$ . The time of observation was the same to within 10% for any set of equal sidereal time intervals.  $\chi^2$  tests were performed on the observed number of events in each  $10^\circ \times 10^\circ$  region along the declination band, and the results were consistent with the hypothesis of isotropy. Also a number of special regions in the sky were tested, and no significant anisotropy was present.

#### Solar Variations.

The arrival at earth of Cosmic ray particles is affected by changes in the atmospheric temperature and pressure which cause changes in the altitude-density relation. These variations are partly erratic, but the influence of the sun on the atmosphere gives rise to certain periodicities. There is a solar diurnal temperature variation, and both a diurnal and a semi-diurnal pressure wave, an annual temperature cycle and also a pronounced annual variation of the diurnal amplitudes. The seasonal modulation of the diurnal waves gives rise to a Fourier component that has

one more cycle/year than the solar variation, hence spurious daily intensity variations are present in sidereal time as well as solar time.

It is interesting to note that several groups working with Mc Cusker in Dublin, Jamaica and Sydney, using M - units\* as detectors, have found large semi-diurnal variations in solar time which appear to be correlated with the semi-diurnal pressure wave at ground. Mc Cusker proposed that the variation in counting rate is caused by a change in the structure of the showers; the large amplitude suggests that this change in shower structure is associated with a tidal motion of the height of the first interaction, and that this interaction occurs at a region where tidal changes in its height could be very large. Below 30 Km diurnal and semi-diurnal pressure changes are small, however above this it is possible that large tidal motions occur. It is most unlikely that the first interaction of proton primaries is in the region where large tidal motions occur since protons have a maximum probability of interacting at about 18 Km. It has recently been suggested<sup>6</sup> however that less than half the primaries with a given energy above  $10^{15}$  are protons, and that the proportion of heavier primaries should increase rapidly with energy above this. The way in which the primary disintegrates on interaction in the upper atmosphere controls the shower structure close to the core. The spread of the core is controlled by the energy with which the nucleons are emitted; if the primary is as big as iron it is possible that several hundred mesons are produced. In this case it is possible that the size of the core stays relatively constant for all shower sizes to which

Mc Cusker's apparatus is sensitive.

Pearson and Butler suggest that a change in the height of the first interaction changes the electron density in the area covered by the nucleon core. With increasing shower size the electron density outside the core becomes sufficient to trigger the M - unit; the core density becomes so large that the M - unit is saturated, therefore for showers greater than a given size the counting rate is no longer sensitive to the first interaction. The large solar variations observed by Mc Cusker imply a tidal amplitude of the 40 Km level of between 3 and 10 Km.

Observed Solar time variations are given in Table 2.

\* An M-unit consists of three small G.M. counters forming the sides of a triangle, the sides being each 20 cms. For an M-unit to record, all three G.M. counters must go off in coincidence; M- units are therefore more sensitive to a high density of particles e.g. the core of an E.A.S.

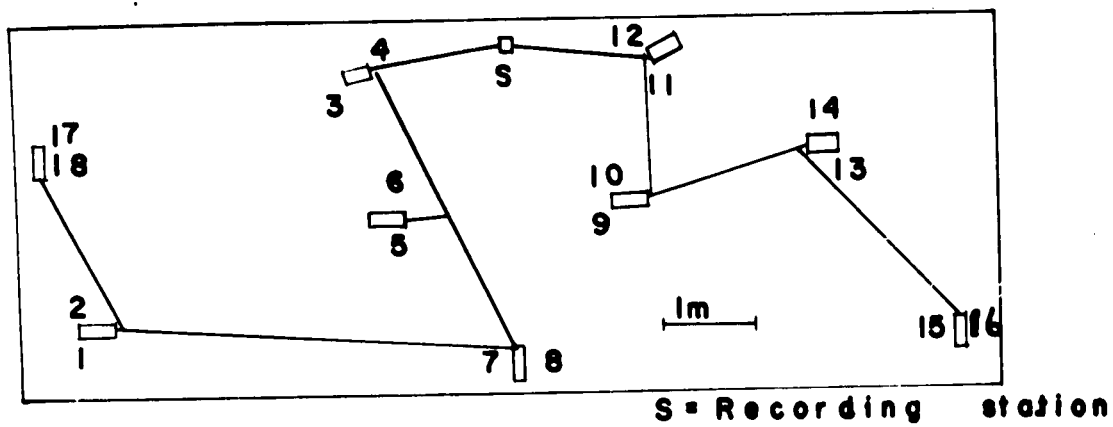
Experiment	Altitude	Total Counts N	Primary Energy e.v.	Amplitude per cent	Time of Max. G.M.T.	P %	*
Cranshaw and Elliot	Near S.L.	3414	$2.10^{16}$	1		92	
		711	$10^{17}$	19.3	1230	0.5	
Cranshaw and Galbraith - I	Near S.L.	71000	$10^{16}$	0.6		51	
		22000	$2.10^{16}$	0.5		87	
		8500	$5.10^{16}$	2.2		37	
		500	$10^{17}$	6.7		56	
Cranshaw and Galbraith - II	Near S.L.	37000	$7.10^{17}$	2.5	1430	0.5	
		7200	$1.5 \times 10^{17}$	4.5	1500	3	
		1900	$2.7 \times 10^{17}$	9.8	1430	1	
		150	$10^{18}$	21.0	1230	18	
McCusker and Wilson	Near S.L.	726	High Density	9	1430		
		120	Showers - 700 particles / m <sup>2</sup>	23	1000		

Table 2. Results of Time Variation Experiments in Solar Time

(Reproduced from Galbraith)

\* P is the probability that the observed amplitude could arise as a result of statistical fluctuations in the sample of N counts.





**Fig.1a Arrangement of GMC containers in the laboratory**

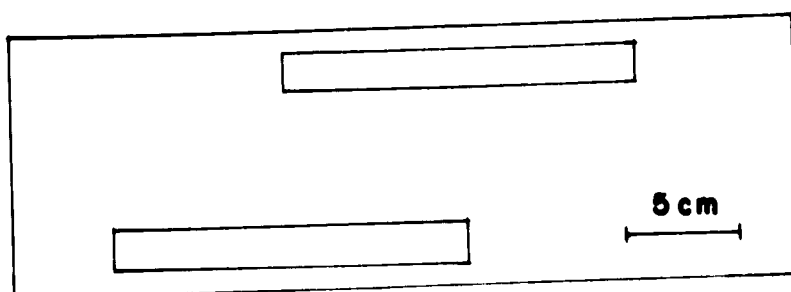


**Fig.1b Arrangement of GMC in containers.**

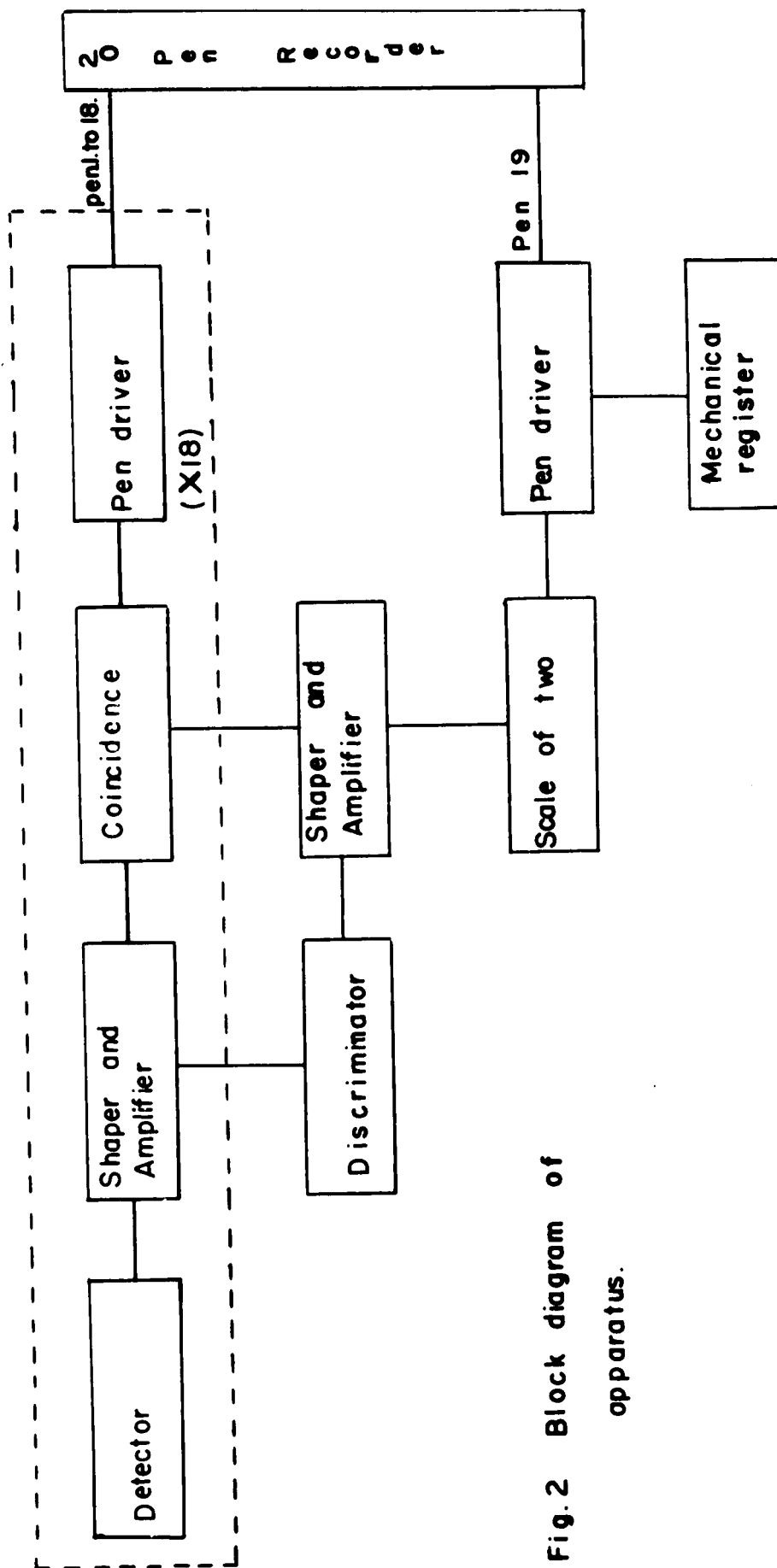


Fig.2 Block diagram of apparatus.

## Experimental Apparatus.

The experiment was carried out both at the University of Alberta Cosmic Ray Station on Sulphur Mountain, Banff, Alberta at an altitude of 2283m and in the penthouse of the Science Building at the University of Alberta, Calgary, at 1086m.

In both Banff and Calgary the apparatus consisted of a horizontal array of eighteen Geiger-Mueller counters each of  $25.8 \text{ cm}^2$  sensitive area grouped in pairs in nine thin aluminum containers. The containers were arranged as in Fig. 1a so that no three counters could be triggered by a horizontal particle moving in a straight line. A shower is defined by a threefold coincidence between any of the eighteen counters. A block diagram of the detecting and recording circuits is given in Fig. 2. Full circuit diagrams are given in reference 7.

Negative pulses from each G.M.C. are first cathode followed by a triode (1/2 12AT7); a series diode (1/2 6AL5) cuts off the positive overshoot before amplification by a 6AQ5. A shunt diode (1/2 6AL5) then reduces the pulse to a uniform height; two outputs "a" and "b" are provided. The "b" outputs from each channel are added and fed to a non-linear amplifier (6AQ5) that amplifies 1, 2, 3-folds and up in the ratio 1:10:100: saturation. After amplification by a 6J6, 1 and 2 fold pulses are eliminated by a series diode (1/2 6AL5). Pulses from 3-folds to 18-folds are limited to a constant height by a shunt diode (1/2 6AL5) and cathode followed by a 6L6. These pulses trigger a uni-vibrator (12AT7) and are cathode followed (6AQ5) to give a "Master Pulse" of constant size.

"The Master Pulse" is brought in coincidence with output "a" in each channel through a 6BN6. If coincidences occur the pulse in each channel is amplified (6AG5) and triggers a thyratron (2D21) which drives a pen of an Esterline-Angus 20 pen recorder (pens 1 - 18).

The "Master Pulse" is also fed to a scale of two (6AL5, 6SN7) after amplification by a 6AG5. The output of the scale of two triggers a thyratron to drive pen 19, and also a mechanical counter. The scale of two helps distinguish between very close showers which could be mistaken for a single shower. Minute and hour signals are fed to pen 20.

### Calculation of the Energy of E.A.S. Detected by the Banff Apparatus.

It is already known<sup>7.</sup> that the densities of particles in an E.A.S. required to cause a 3 - 6 fold, 7 - 12 fold or 13 - 18 fold event in the Banff apparatus are in the range 30 - 140 particles /m<sup>2</sup>, 140 - 420 particles /m<sup>2</sup> and 420 and upwards particles /m<sup>2</sup> respectively. To calculate the total energy of the shower, the energy of the e.m. component was first calculated, and from this, using the relation between the energies of the e.m.,  $\mu$ , and N- components, the total energy was calculated.

The density of the e.m. component of the shower varies radially, and with the total number of particles in the shower, following the relation,<sup>8.</sup>

$$\rho(N,r) = \frac{0.4 N}{r_1^2} \left( \frac{r_1}{r} \right)^{0.75} \left( \frac{r_1}{r+r_1} \right)^{3.25} \left( 1 + \frac{r}{11.4 r_1} \right)$$

Where  $r$  is the radial distance from the axis of the shower,  $N$  is the total number of electrons in the shower and  $r_1$  is the Molière unit.\*

\*  $r_1$ , the Molière unit. The lateral distance an electron is scattered

in traversing a longitudinal distance of one radiation length is approximately  $1/4$  radiation length or  $9.5g \text{ cm}^{-2}$  i.e. about 79 m at sea level, or 116.4 m at 2283 m. This unit of length is denoted by  $r_1$ , the characteristic or scattering length.

This is a close approximation to the theoretical expressions derived by Kamata and Nishimura for e.m. cascades having  $s = 1.25$ .

$\rho(N, r)$  was calculated for values of  $r$  from 10 m to 200 m for values of  $N$  of  $10^5$  particles to  $5 \cdot 10^7$  particles, and the results are shown in Table 3.

Graphs were plotted, for each value of  $N$ , of  $r$  against particle density (Figs 3a, 3b and 3c) and in each case the radii corresponding to particle densities of 30 particles /  $m^2$ , 140 particles /  $m^2$  and 420 particles /  $m^2$  were noted; from these radii the area of the part of the shower capable of producing 3-6, 7-12 and 13-18 fold events were calculated and are given in Table 4.

It can be assumed that the number spectrum will be the same as the energy spectrum since showers of the same energy contain the same number of particles. The number frequency spectrum was plotted for values of  $\gamma$ , the exponent of the number spectrum, equal to 1.5 and 1.9 (fig. 4) using an arbitrary scale for frequency, and the frequencies corresponding to the required values of  $N$  were obtained.

By multiplying the relative frequency by the area corresponding to each value of  $N$  for 3-6, 7-12 and 13-18 folds we get an expression which is a function of the probability of a 3-6, 7-12 or 13-18 fold event being caused by a shower containing  $N$  particles. Frequency x Area was calculated for each value of  $N$  for 3-6, 7-12 and 13-18 folds, for  $\gamma = 1.5$  (Table 5) and  $\gamma = 1.9$  (Table 6).

When these values were plotted (Figs. 5 and 6) maxima were found at

<u>Distance</u>	$N=10^5$	$N=3 \cdot 10^5$	$N=5 \cdot 10^5$	$N=10^6$	$N=3 \cdot 10^6$	$N=5 \cdot 10^6$	$N=10^7$	$N=5 \cdot 10^7$
10	15.6	46.8	78.0	156.4	468	780	1,564	7,800
30	3.9	11.8	19.7	39.4	118	197	394	1,970
70	1.0	3.0	4.9	10.0	29.6	49	99	490
100		1.4	2.4	4.7	14.2	24	47	240
150				1.85	5.5	9	18	90
200					2.7	4	9	40

Table 3. Particle Density (N,r), For Different Values of r and N,  
in Particles / m<sup>2</sup>

<u>Value of N</u>	$10^5$	$3 \times 10^5$	$5 \times 10^5$	$10^6$	$3 \times 10^6$	$5 \times 10^6$	$10^7$	$5 \times 10^7$
<u>Area For 3-6</u>	38	687	1,504	3,538	12,654	20,156	34,286	104,902
<u>Area For 7-12</u>			113	503	2,242	4,058	8,103	29,754
<u>Area For 13-18</u>				28.2	490	1,220	2,827	20,096

Table 4. Area Capable of Producing 3-6, 7-12 And 13-18 Folds For  
Different Values of N.

Fig. 3a.

Distance R from axis  
VS particle density for  
 $N - 10^5$ .

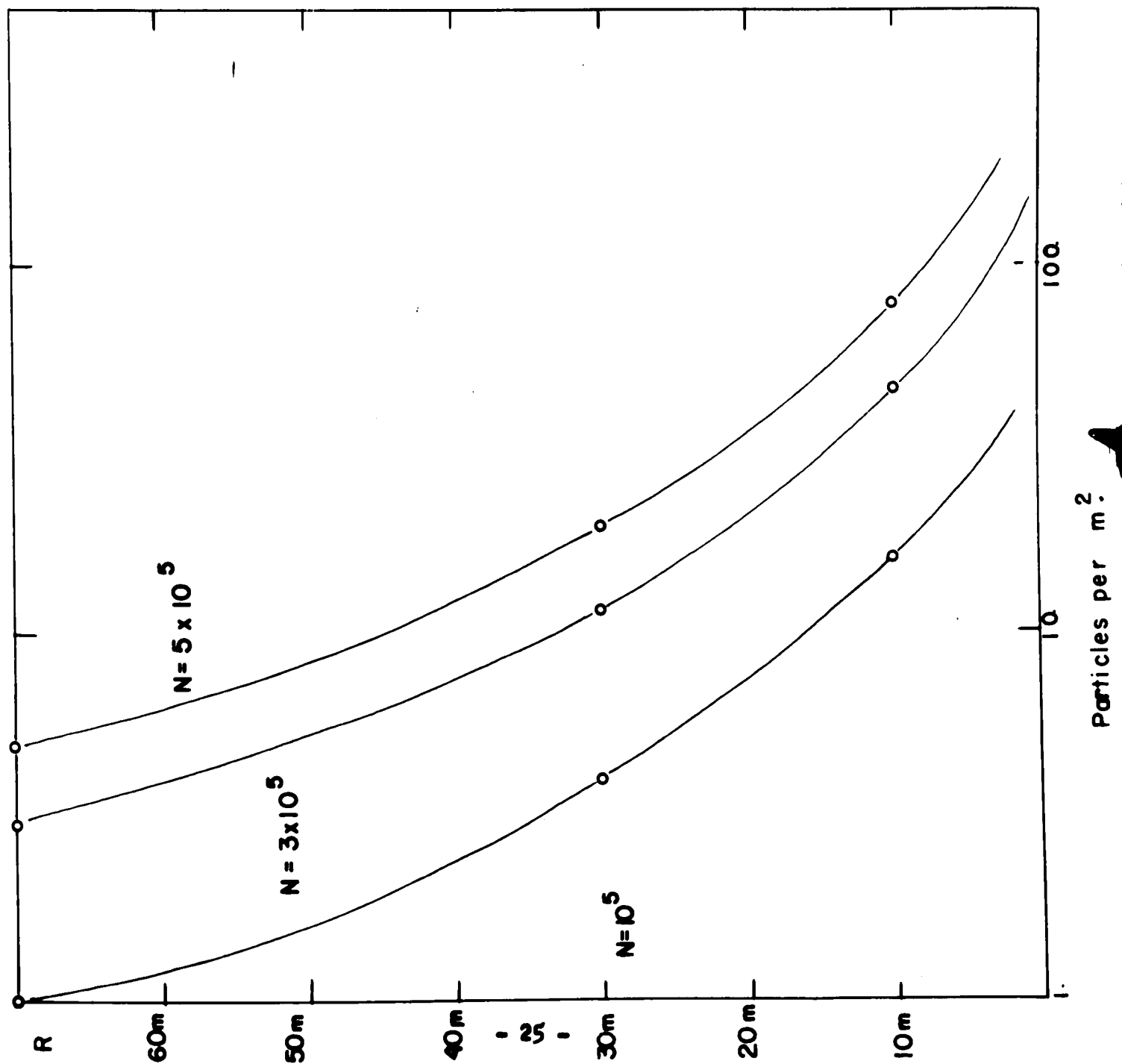




Fig. 3 b

Distance R from axis VS particle  
density for  $N = 10^6$

$N = 5 \times 10^6$

$N = 3 \times 10^6$

$N = 10^6$

Particles per  $m^2$ .

120m

100m

80m

20

60m

40m

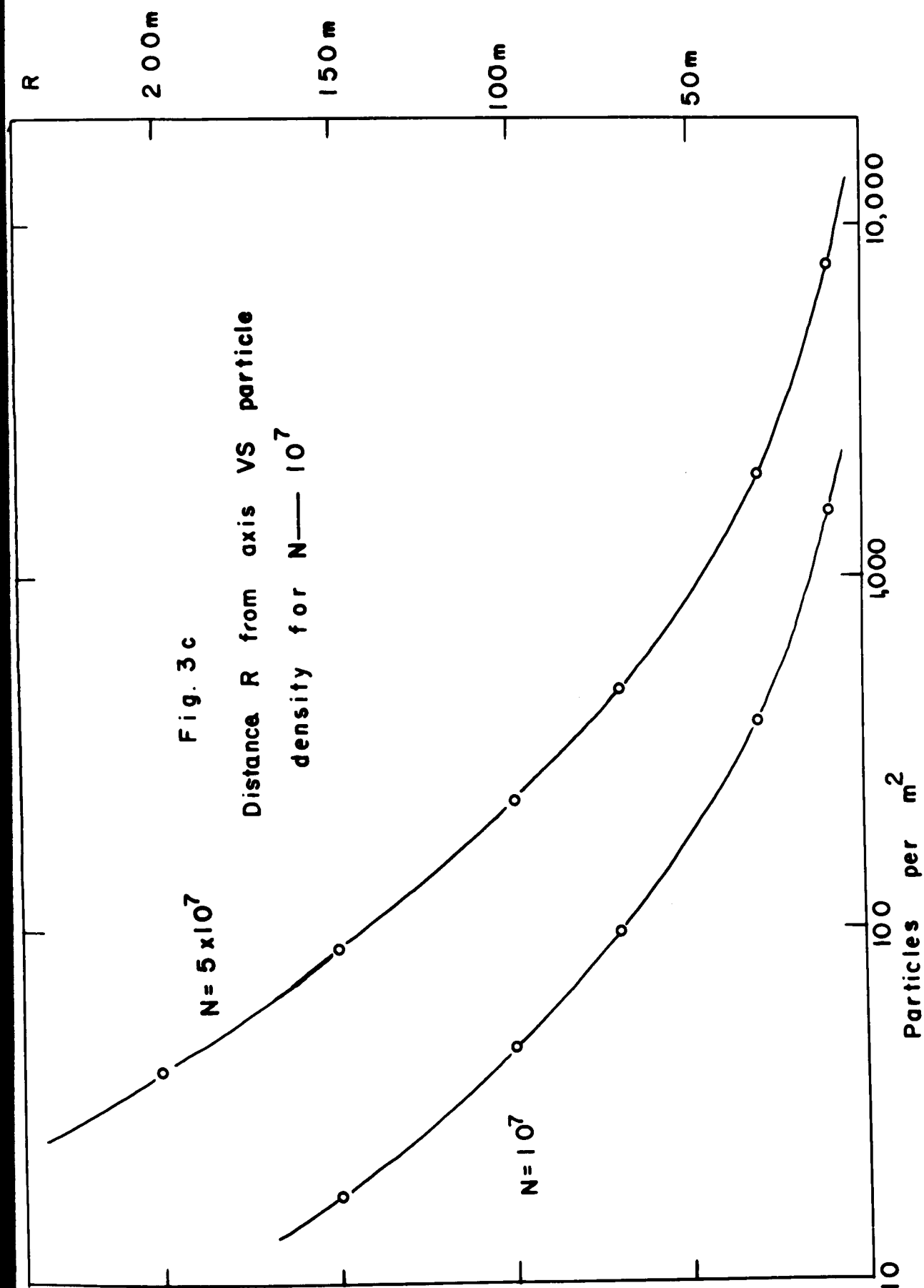
20m

1,000

100

10





<u>Value of N</u>	$10^5$	$3 \times 10^5$	$5 \times 10^5$	$10^6$	$3 \times 10^6$	$5 \times 10^6$	$10^7$	$5 \times 10^7$
<u>Relative Frequency</u>	$10^5$	$2.4 \times 10^4$	$1.18 \times 10^4$	$4.6 \times 10^3$	$1.15 \times 10^3$	$5.5 \times 10^2$	$2.2 \times 10^2$	$2.57 \times 10^1$
<u>Frequency x Area For 3-6</u>	$3.8 \times 10^6$	$1.63 \times 10^7$	$1.77 \times 10^7$	$1.64 \times 10^7$	$1.3 \times 10^7$	$1.1 \times 10^7$	$7.5 \times 10^5$	$2.7 \times 10^6$
<u>Frequency x Area For 7-12</u>			$1.33 \times 10^6$	$2.34 \times 10^6$	$2.58 \times 10^6$	$2.23 \times 10^6$	$1.78 \times 10^6$	$7.6 \times 10^5$
<u>Frequency x Area For 13-18</u>				$1.31 \times 10^5$	$5.64 \times 10^5$	$6.7 \times 10^5$	$6.22 \times 10^5$	$5.16 \times 10^5$

Table 5. Frequency x Area For 3-6, 7-12 and 13-18 Folds with  $\gamma = 1.5$

<u>Value of N</u>	$10^5$	$3 \times 10^5$	$5 \times 10^5$	$10^6$	$3 \times 10^6$	$5 \times 10^6$	$10^7$	$5 \times 10^7$
<u>Relative Frequency</u>	$5 \times 10^6$	$6.8 \times 10^5$	$2.7 \times 10^5$	$6.3 \times 10^4$	$7.8 \times 10^3$	$3.1 \times 10^3$	$7.9 \times 10^2$	$3.4 \times 10^1$
<u>Frequency x Area For 3-6</u>	$1.9 \times 10^8$	$4.6 \times 10^8$	$4.06 \times 10^8$	$2.23 \times 10^8$	$9.9 \times 10^7$	$6.2 \times 10^7$		
<u>Frequency x Area For 7-12</u>			$3.05 \times 10^7$	$3.17 \times 10^7$	$1.75 \times 10^7$	$1.25 \times 10^7$	$6.4 \times 10^6$	
<u>Frequency x Area For 13-18</u>				$1.7 \times 10^6$	$3.82 \times 10^6$	$3.76 \times 10^6$	$2.23 \times 10^6$	$6.8 \times 10^5$

Table 6. Frequency x Area For 3-6, 7-12 and 13-18 with  $\gamma = 1.9$

$N=3.6 \times 10^5$  for 3-6 folds,  $N=8.10^5$  for 7-12 folds and  $N=3.3 \times 10^6$  for 13-18 folds for  $\gamma=1.9$ ; for  $\gamma=1.5$  maxima were at  $N=6.5 \times 10^5$  for 3-6 folds,  $N=2.15 \times 10^6$  for 7-12 folds and  $N=5.0 \times 10^6$  for 13-18 folds. These values of  $N$  indicate the most probable number of particles in the appropriate showers.

The energy of the e.m. component is given approximately by the formula

$$E_0 \approx 0.2 N \cdot 10^9 \text{ e.v.}$$

Where  $E_0$  is the total energy carried by the e.m. component. Assuming  $\gamma=1.9$  we get:-

For 3-6 folds	the total e.m. energy is	$7.2 \times 10^{13}$ e.v.
7-12 folds	" " " " "	$1.6 \times 10^{14}$ e.v.
13-18 folds	" " " " "	$6.6 \times 10^{14}$ e.v.

Assuming  $\gamma=1.5$  we get:-

For 3-6 folds	the total e.m. energy is	$1.3 \times 10^{14}$ e.v.
7-12 folds	" " " " "	$4.3 \times 10^{14}$ e.v.
13-18 folds	" " " " "	$1.0 \times 10^{15}$ e.v.

#### Energy Distribution Among Shower Components.

Of the three components constituting an E.A.S., the  $\mu$ -meson component carries the largest part of the energy, while the e.m. and the nucleonic components both carry approximately the same energy, each about one eighth of the total shower energy. By integration over the energy spectrum, one can obtain the average total energy of the  $N$  - component; within the accuracy of these calculations, the resultant energy is equal to the energy carried by the e.m. component,  $2N \cdot 10^8$  e.v.

This result seems to be independant of shower size and elevation, although it refers only to statistical averages: individual showers exhibit considerable fluctuations.

In an average shower of  $10^6$  charged particles, which is approximately the size of showers detected by the Banff apparatus, about 17% are  $\mu$ -mesons; their mean energy computed from

$$N_{\mu}(>E, N) = 1.7 \times 10^5 \left( \frac{2}{E+2} \right)^{1.37} \left( \frac{N}{10^6} \right)^{0.75}$$

is 5.4 Bev. The mean photon-electron energy per electron in the shower is only 0.2 Bev., hence the energy carried by the  $\mu$ -meson component is about five and a half times that of the e.m. component. The energy constitution of the shower is therefore:-

1 part	from the e.m.	component
1 part	from the N -	component
5 1/2 parts	from the $\mu$ -	component

This situation is a consequence of the long range of  $\mu$ -mesons and the comparatively rapid absorption of the other components.

To obtain the total energy of the shower, the energy of the e.m. component must be multiplied by 7.5. This means that for the Banff apparatus, assuming a value for  $\gamma$  of 1.9, the shower energies are:-

3-6	fields	$5.4 \times 10^{14}$ e.v.
7-12	fields	$1.2 \times 10^{15}$ e.v.
13-18	fields	$4.95 \times 10^{15}$ e.v.

Assuming a value for  $\gamma$  of 1.5, the shower energies are:-

3-6	fields	$9.75 \times 10^{14}$	e.v.
7-12	fields	$3.23 \times 10^{15}$	e.v.
13-18	fields	$7.5 \times 10^{15}$	e.v.

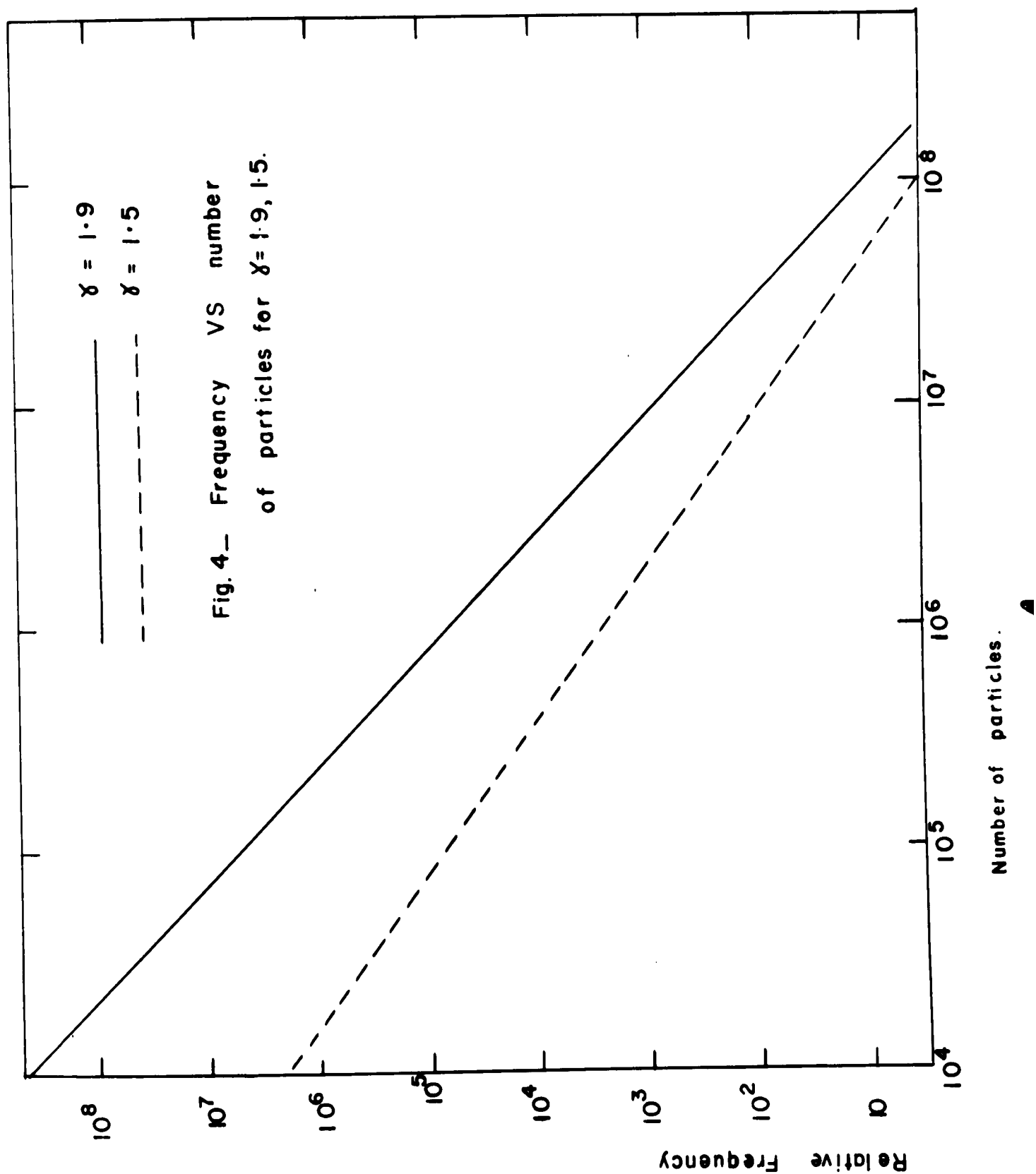


Fig. 4— Frequency VS number  
of particles for  $\chi=1.9, 1.5$ .

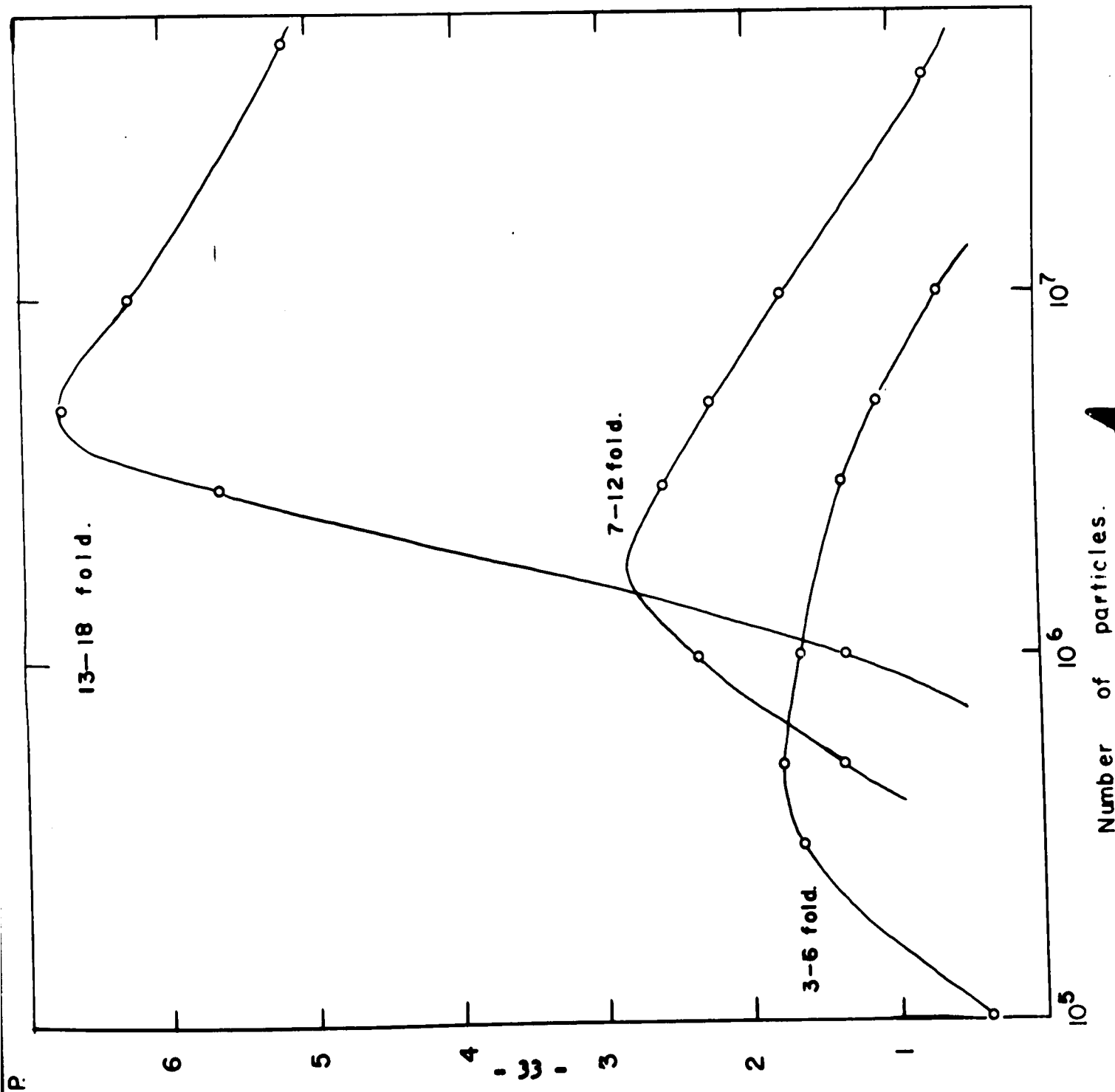


Fig. 5—  
 Probability  $P$  VS  
 number of particles  
 for 3-6, 7-12, and 13-18  
 folds with  $\gamma = 1.5$ .



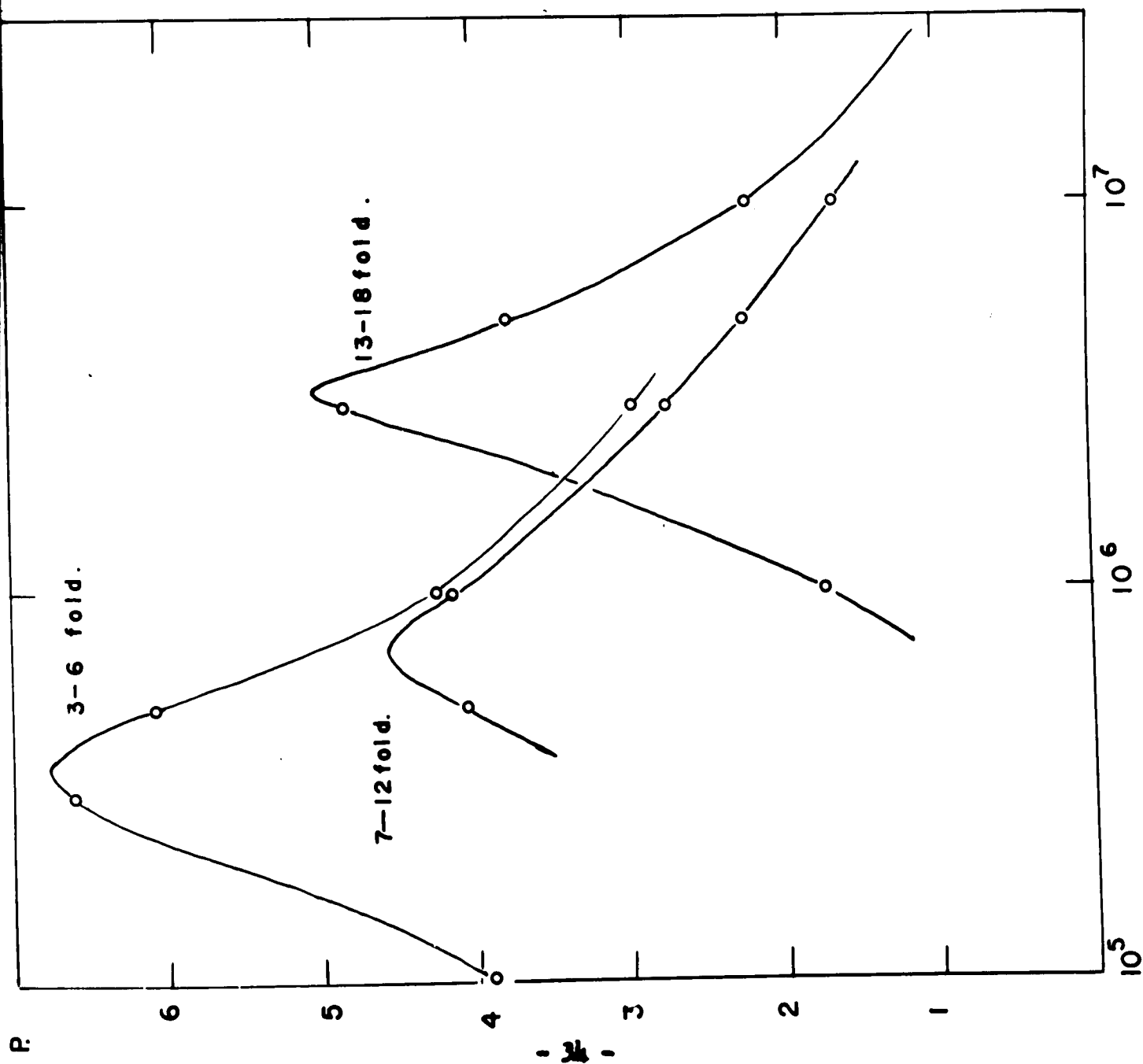


Fig. 6 —

Probability  $P$  VS number  
of particles for 3-6,  
7-12 and 13-18 folds  
with  $\gamma = 1.9$ .

## Analysis of the Data

Results from the shower experiment are continuously recorded on an Esterline-Angus 20- pen recorder, pens 1-18 recording the individual counters, and pen 20 recording G.M.T. with marks every minute and every hour. Each event is counted to determine the multiplicity, and the results are tabulated for each day as shown in Fig. 7.

### (a) Time Variations.

Results for the shower experiment in Banff have been analysed for data from July 1st 1959 until the end of June 1961. Results from the Calgary experiment have been analysed for data from November 1959 to September 1960.

All the charts were first analysed in solar time, and then re-analysed in sidereal time. Sidereal time for 00.00 G.M.T. on the first of each month of the year was obtained from "The Star Almanac for Land Surveyors", for Banff and for Calgary; a further graph was plotted giving the correction to be applied to this sidereal time for any subsequent time during the month. Using this method to establish the correct sidereal time at the beginning and end of each chart, and by shifting the sidereal hour position 10 seconds every solar hour, the results were recorded in sidereal time in the same way that solar data were recorded in Fig. 7. Totals for the 24 1-hour periods were obtained, and for Banff normalised to 545 days and for Calgary to 207 days. The hourly totals were obtained for 3-6 folds, 7-12 folds, 13-18 folds and total counts in each case. To obtain the best sine wave through these points the following method was used:-

DATE: JULY 11, 1960

CHART: No. 168

STATION: BANFF

REMARKS

TIME	3	4	5	6	3-6	7	8	9	10	11	12	7-12	13	14	15	16	17	18	18 1/2	TOTAL	PRES.
0-1	7	4	3		14	1			1			2				1				16	770.3
2	7	1	4	1	13		1		1			2			1					16	770.4
3	11	5	1	1	18											1				19	770.9
4	10	5	1	2	18	1	1		1			3	1		1				2	23	771.1
5	10	4		2	16															16	771.7
6	12		1	1	14															14	771.7
7	8	2	3	1	14								2						2	16	772.0
8	6	2	1	3	12				1			1	1						1	14	772.1
9	14	3	2	1	20		2					2								22	772.2
10	16	3	3	3	25		1				1	2		1				1		28	772.2
11	13	3	3	2	21		2					2			1					24	772.3
12	10	2	3		15	1						1								16	772.6
13	15	4	1	3	23		1					2								25	773.2
14	6	3	5	1	15	1	1	1				3								18	773.8
15	16	5		1	22		2			1		3								25	774.2
16	9	7	4		20															20	774.8
17	8	1	2		11		2		1		1	4								15	775.1
18	13	1		4	18	1				1		2								20	775.4
19	9	4	1		14		1	1				2	1	1					2	18	775.4
20	11	2	2	4	19	1						1								20	775.5
21	6	3	1	1	11	1	1					2			1				1	14	775.8
22	9	1			10									1					1	11	776.4
23	11	1	3	1	16		2			2		4	1	1					2	22	776.4
24	11	7	2		20				1		1	2								22	776.7
TOTAL	248	73	46	32	399	7	17	3	7	4	2	40	6	4	1	3		1	15	454	773.9

Fig. 7 Sheet to record the data.

for hourly counts  $x_0, x_1, \dots, x_{23}$  corresponding to the 24 hourly intervals, the first harmonic of the wave is given by

$$F(\theta) = A_0 + A \sin \theta - B \cos \theta$$

expressing hours in degrees so that 24 hours corresponds to  $360^\circ$ , and  $F(\theta)$  is the expected number of counts in a given hourly interval, and  $A_0$  is the mean number over all intervals. The required conditions are met by values of A and B of  $-1/12 \sum (a)$  and  $-1/12 \sum (b)$  respectively, where:-

$$\begin{aligned} \sum (a) = & \sin \pi/12 ( -x_1 - x_{11} + x_{13} + x_{23} ) \\ & \sin 2\pi/12 ( -x_2 - x_{10} + x_{14} + x_{22} ) \\ & \sin 3\pi/12 ( -x_3 - x_9 + x_{15} + x_{21} ) \\ & \sin 4\pi/12 ( -x_4 - x_8 + x_{16} + x_{20} ) \\ & \sin 5\pi/12 ( -x_5 - x_7 + x_{17} + x_{19} ) \\ & \sin 6\pi/12 ( -x_6 \qquad \qquad + x_{18} ) \end{aligned}$$

$$\begin{aligned} \sum (b) = & \sin \pi/12 ( x_5 - x_7 - x_{17} + x_{19} ) \\ & \sin 2\pi/12 ( x_4 - x_8 - x_{16} + x_{20} ) \\ & \sin 3\pi/12 ( x_3 - x_9 - x_{15} + x_{21} ) \\ & \sin 4\pi/12 ( x_2 - x_{10} - x_{14} + x_{22} ) \\ & \sin 5\pi/12 ( x_1 - x_{11} - x_{13} + x_{23} ) \\ & \sin 6\pi/12 ( x_0 \qquad -x_{12} ) \end{aligned}$$

The amplitude of the sine wave is given by  $(A^2 + B^2)^{1/2}$ , and the maximum of the sine wave occurs at a value of  $\Theta$  given by  $\tan^{-1} (-A/B)$ .

Each set of results for solar and sidereal time was also grouped into 3-hour intervals giving three sets of results for the three possible groupings. A  $\chi^2$  test was performed on each group, assuming a straight line was the best fit to the data, and the grouping which gave the worst fit to a straight line was noted in each case.  $\chi^2$  tests were also performed on the 1-hour totals assuming (1) a straight line was the best fit (2) the calculated sine wave was the best fit. The corresponding probabilities and amplitudes and maxima times for the sine waves are recorded in table 7. For each component of Banff solar, Banff sidereal and Calgary sidereal data a graph was plotted of mean hourly counts for each of the 24 hour periods as a percentage deviation from the mean count for the 24 hours; in each case a graph of the 3-hour grouping which gave the worst fit to a straight line was plotted, again as a deviation from the mean. The possible statistical error was indicated on each graph. Banff sidereal 3-6 fold, 7-12 fold, 13-18 fold and total variations are given in Figs. 8, 9, 10 and 11 respectively. Calgary sidereal 3-6 fold, 7-12 fold, 13-18 fold and total variations are given in Figs. 12, 13, 14 and 15 respectively. Banff Solar 3-6 fold, 7-12 fold, 13-18 fold and total variations are given in Figs. 16, 17, 18 and 19 respectively.

#### (b) Density Spectrum.

The total number of events of each multiplicity 3-fold to 18-fold have been obtained<sup>7</sup> for the Banff shower experiment for the period July 1st 1959 to August 1960. These were normalised to 100,000 events. Results from August 1960 up to the end of June 1961 have now been calculated for each multiplicity and again normalised to 100,000 events. The number of events

	Prob. of Straight Line	Prob. of Sine Wave	Prob. of Best 3-Hour	Prob. of Worst 3-Hour	Ampl. of Sine Wave	Time of Max.	Ampl. Statistical Error
(a)							
3-6	.16	.31	.37	.011	.6%	04.53GMT	1.7%
7-12	.62	.76	.775	.40	1.4%	12.40GMT	4.3%
13-18	.22	.27	.615	.215	1.6%	10.11GMT	8.0%
Total.	.14	.22	.30	.019	.5%	05.33GMT	1.45%
(b)							
3-6	.76	.81	.61	.40	.25%	13.37LST	1.25%
7-12	.58	.92	.81	.24	.8%	20.20LST	2.2%
13-18	.038	.04	.68	.30	.9%	07.30LST	8.2%
Total.	.81	.83	.75	.33	.15%	13.03LST	1.07%
(c)							
3-6	.10	.59	.05	.02	2.7%	13.47LST	5.4%
7-12	.685	.83	.55	.20	3.6%	17.25LST	10.8%
13-18	.23	.42	.47	.05	9.3%	01.49LST	26.7%
Total.	.11	.48	.04	.02	2.0%	14.05LST	4.6%

Table 7. Probabilities of Data Representing A Straight Line or A Sine Wave  
For the Various Components

(a) Banff Solar                      (b) Banff Sidereal                      (c) Calgary Sidereal

of each multiplicity are nearly identical with those obtained by Dionne. The two years results have been combined and normalised to 100,000 events, and are given in table 8 along with the statistical error in the number of showers (normalised) and the predicted number of showers to be expected if  $\gamma$  is assumed to vary from 1.4 for 3-fold showers to 2.0 for 18-fold showers. The numbers were obtained<sup>7</sup> by assuming for multiplicities 3, 4 and 5 a value of  $\gamma=1.4$ ; for multiplicities 5, 6, 7 and 8,  $\gamma = 1.5$  was assumed; for multiplicities 8, 9, 10 and 11,  $\gamma = 1.6$  was assumed; for multiplicities 11, 12, 13 and 14,  $\gamma = 1.8$  was assumed, and for multiplicities 14, 15, 16, 17 and 18,  $\gamma = 2.0$  was assumed. The values of  $R(\gamma, n)$  were normalised so that  $R(1.4, 5) = R(1.5, 5)$ ,  $R(1.5, 8) = R(1.6, 8)$ ,  $R(1.6, 11) = R(1.8, 11)$  and  $R(1.8, 14) = R(2.0, 14)$ ; these values were then normalised to 100,000 events.

In Fig. 20 the experimental number of showers is plotted against the expected number of showers for  $\gamma=1.4, 1.5$  and  $1.6$ . In Fig. 21 the experimental number of showers is plotted against the expected number assuming a varying  $\gamma$ , from table 8.

### (c) Baremeter Coefficient

A mechanical register is connected to the scale of two in the shower circuit so that it records every second event; the mean hourly rate for each day has been recorded since December 1959 against the mean pressure for that day. Fig. 22 shows the E.A.S. rate in counts per hour plotted against the daily mean pressure in mb. for a wide pressure range during the period December 1959 to July 1960, and the best line has been drawn through these points.

<u>n</u>	<u>Experimental No. of Showers</u>	<u>Error in No. of Showers</u>	<u>Predicted No. of Showers</u>	<u>Assumed <math>\gamma</math></u>
3	51,338	140.6	50,587.8	1.4
4	19,412	86.3	20,011.8	1.4
5	10,070	62.3	10,293.5	1.4
6	5,894	47.7	5,919.4	1.5
7	3,755	38.1	3,752.2	1.5
8	2,504	31.2	2,544.7	1.5
9	1,760	26.2	1,777.5	1.6
10	1,333	22.7	1,293.6	1.6
11	930	18.8	971.8	1.6
12	708	16.5	726.9	1.8
13	582	15.0	555.1	1.8
14	476	13.5	435.7	1.8
15	373	11.9	333.9	2.0
16	302	10.7	280.2	2.0
17	261	10.0	231.1	2.0
18	302	10.7	284.8	2.0

**Table 8    Experimental Number of Showers and Expected Number of  
Showers Assuming A Variable  $\gamma$  .**



(d) Temperature Coefficient

The monthly mean temperatures for Banff were obtained from the Meteorological Branch, Department of Transport, Canada for the months July 1960 to July 1961, and these are plotted against the corresponding months in Fig. 23a and Fig. 24a. For each of these months the mean daily number of showers for 3-6 feld, 7-12 feld, 13-18 feld and total showers were calculated, and corrected for pressure using a baremeter coefficient of  $- 1.0\% / \text{mb.}$ : the 3-6 feld and 7-12 feld mean daily rates are plotted against the corresponding months in Fig. 23b and Fig. 23c; the 13-18 feld and total mean daily rates are plotted in Fig. 24b and Fig. 24c.

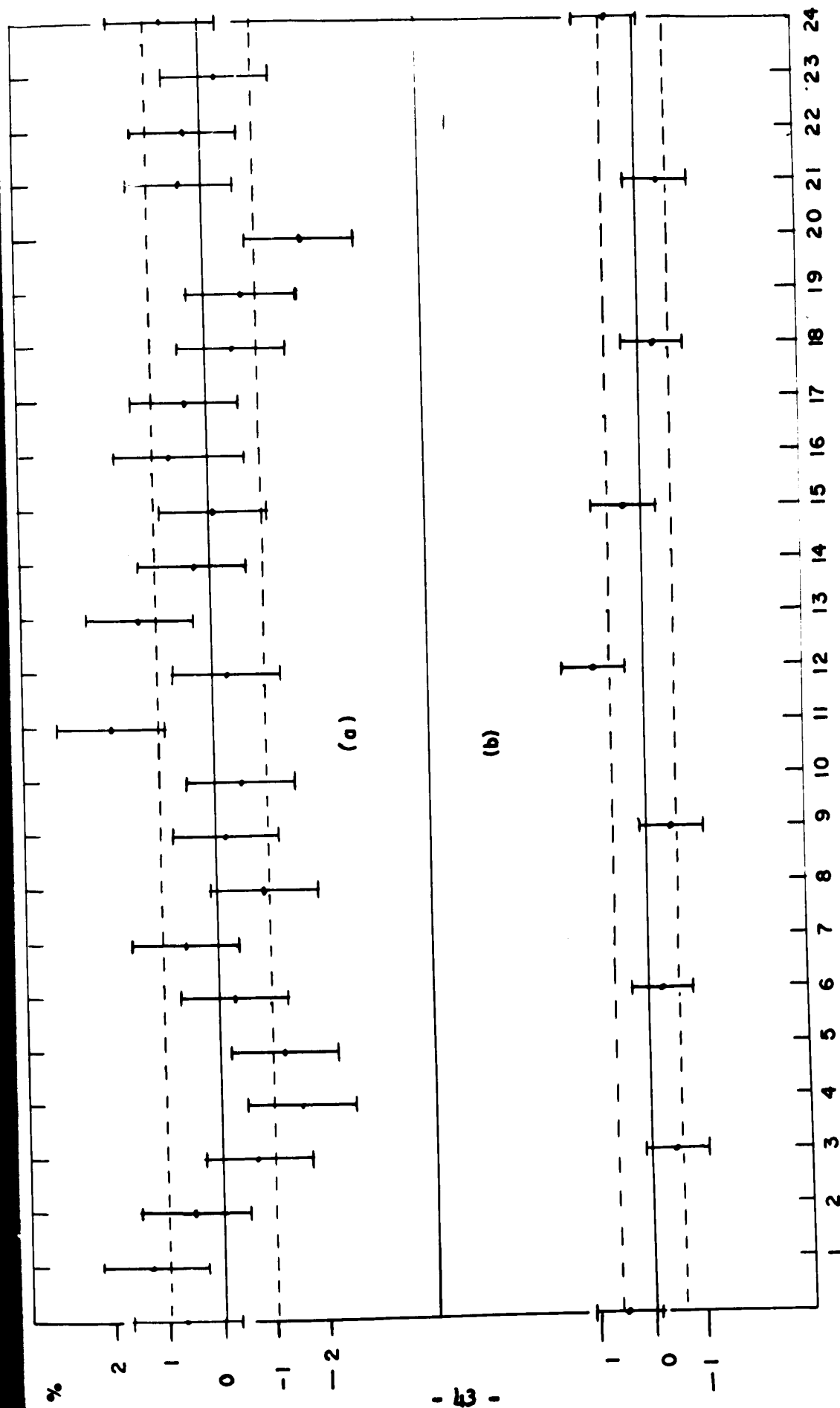


Fig. 8--% Deviation from mean rate for Banff 3-6 folds LST

for (a) 1-hour intervals (b) 3-hour intervals.

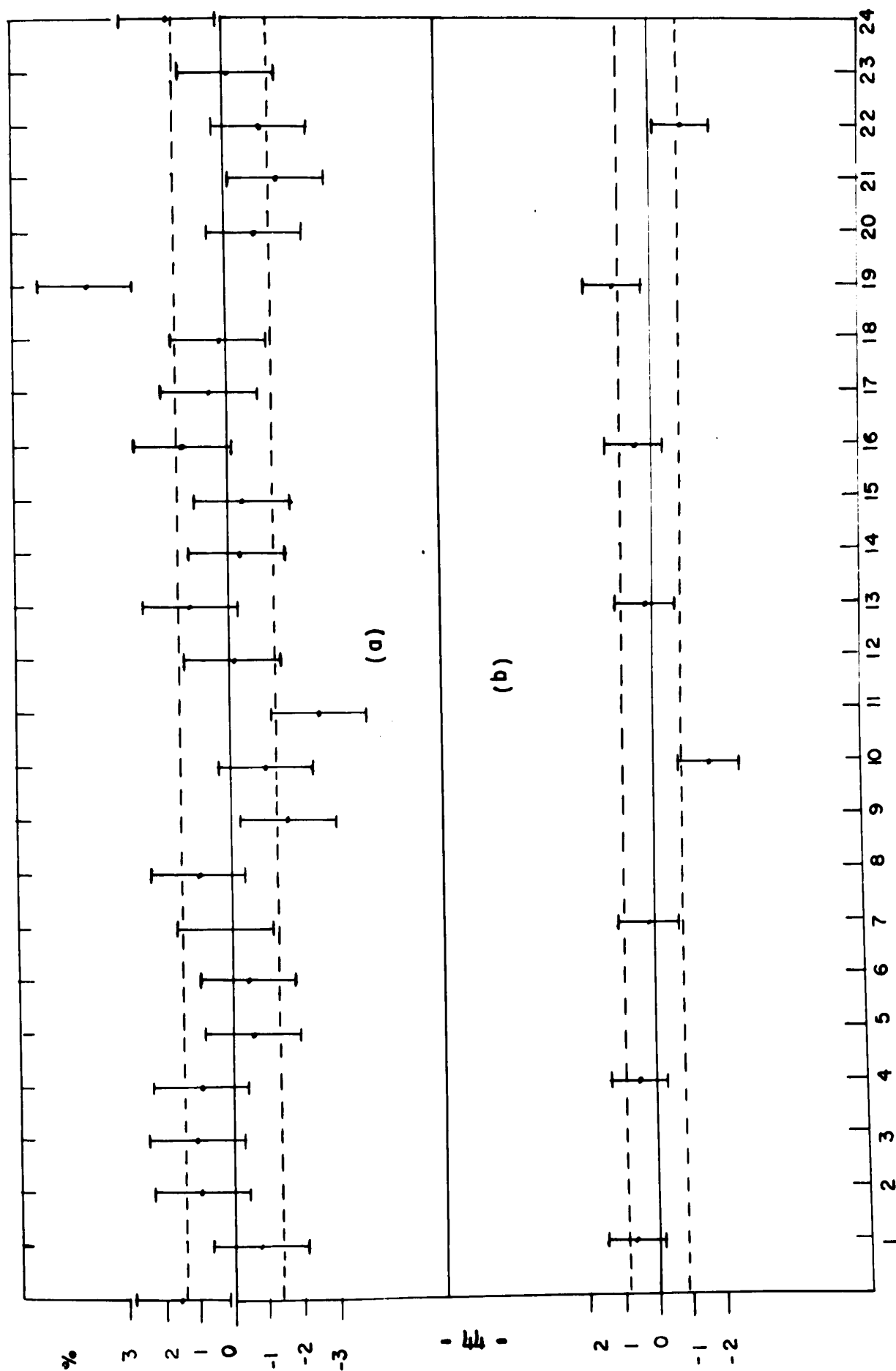


Fig. 9— %Deviation from mean rate for Banff 7-12 folds VS LST for  
 (a) 1— hour intervals (b) 3—hour intervals.

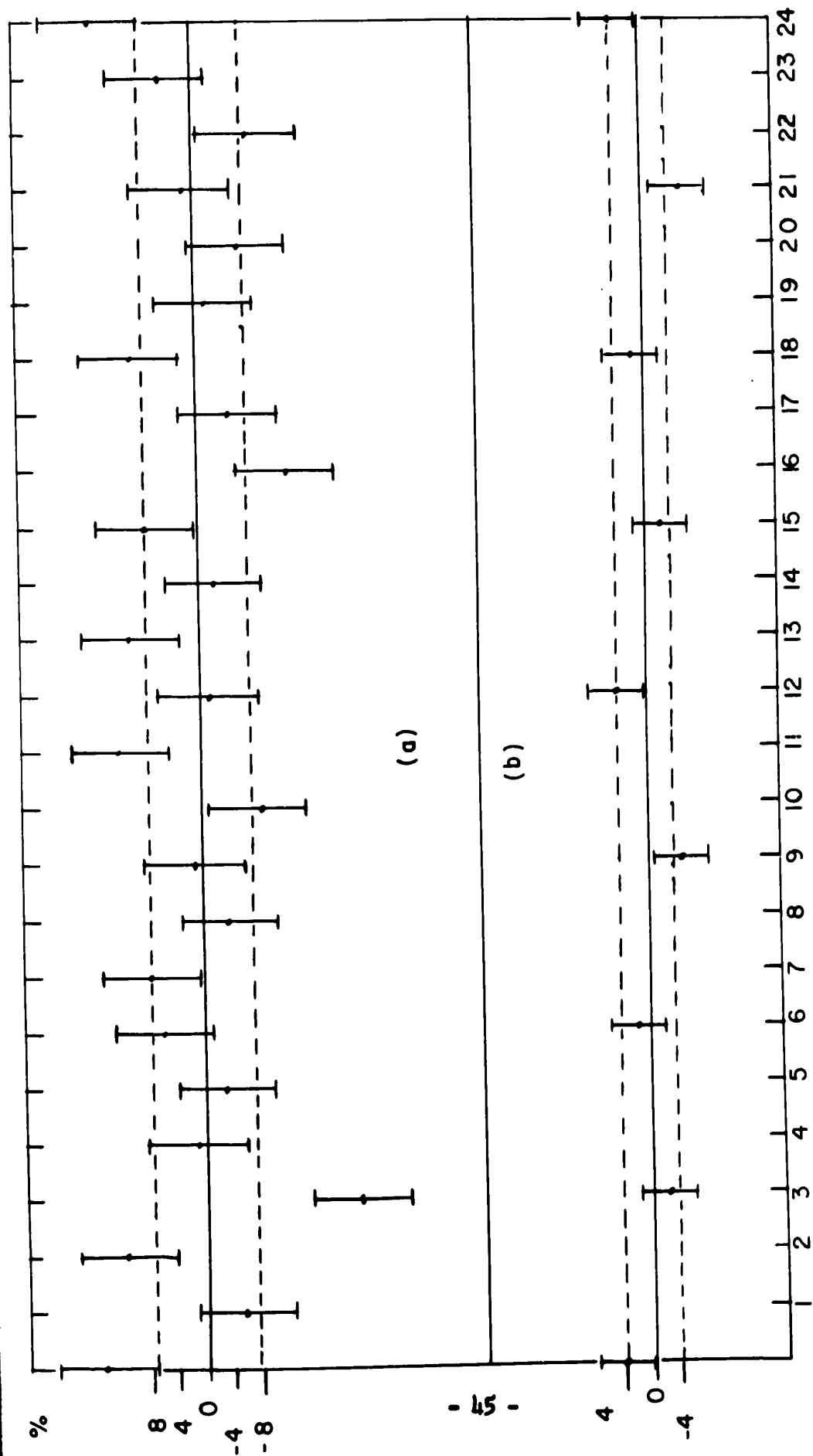


Fig. 10 - % Deviation from mean rate for Banff 13-18 folds VS LST for

(a) 1-hour intervals (b) 3-hour intervals.

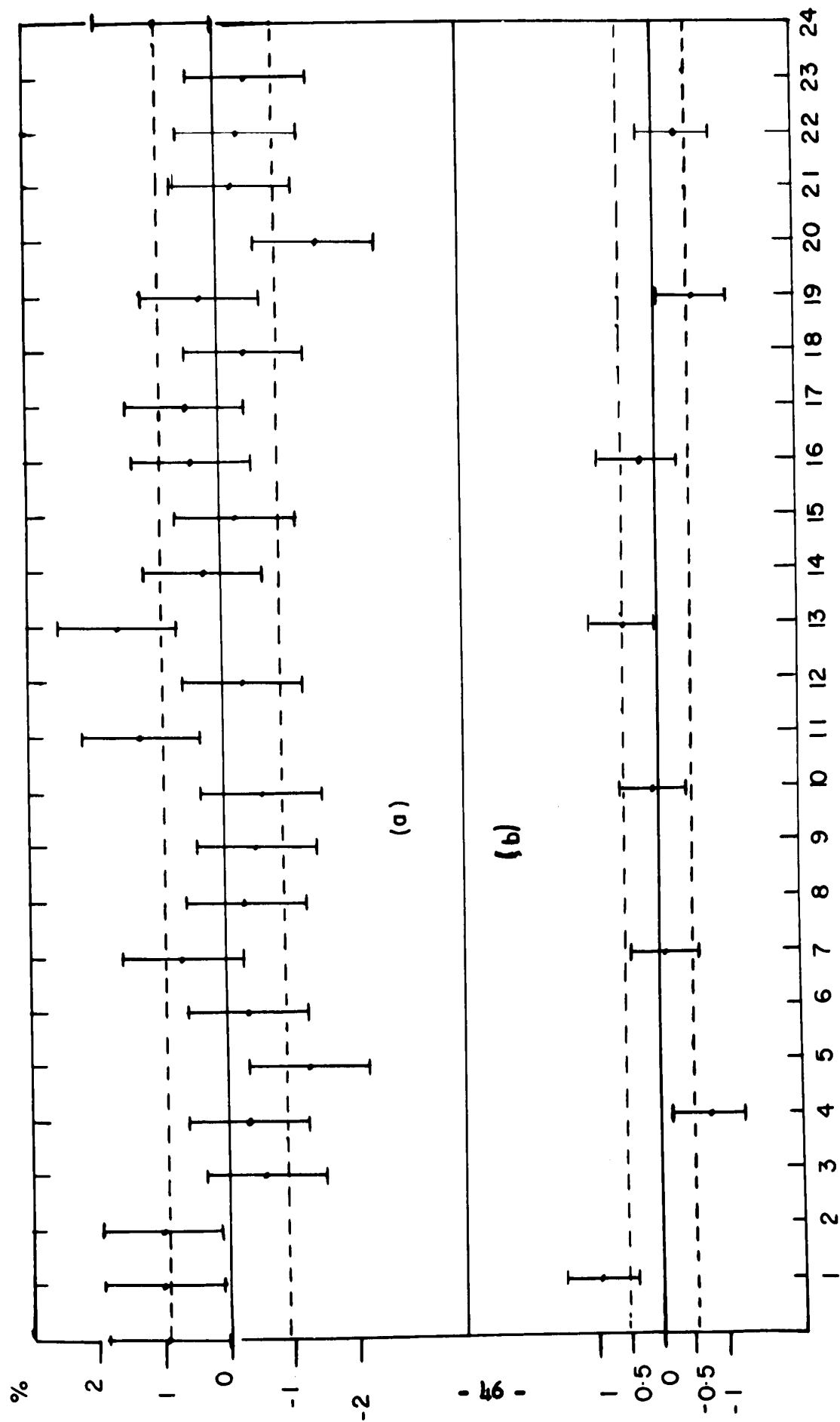


Fig. 11 - % Deviation from mean total rate for Banff VS LST for  
 (a) 1-hour intervals (b) 3-hour intervals.

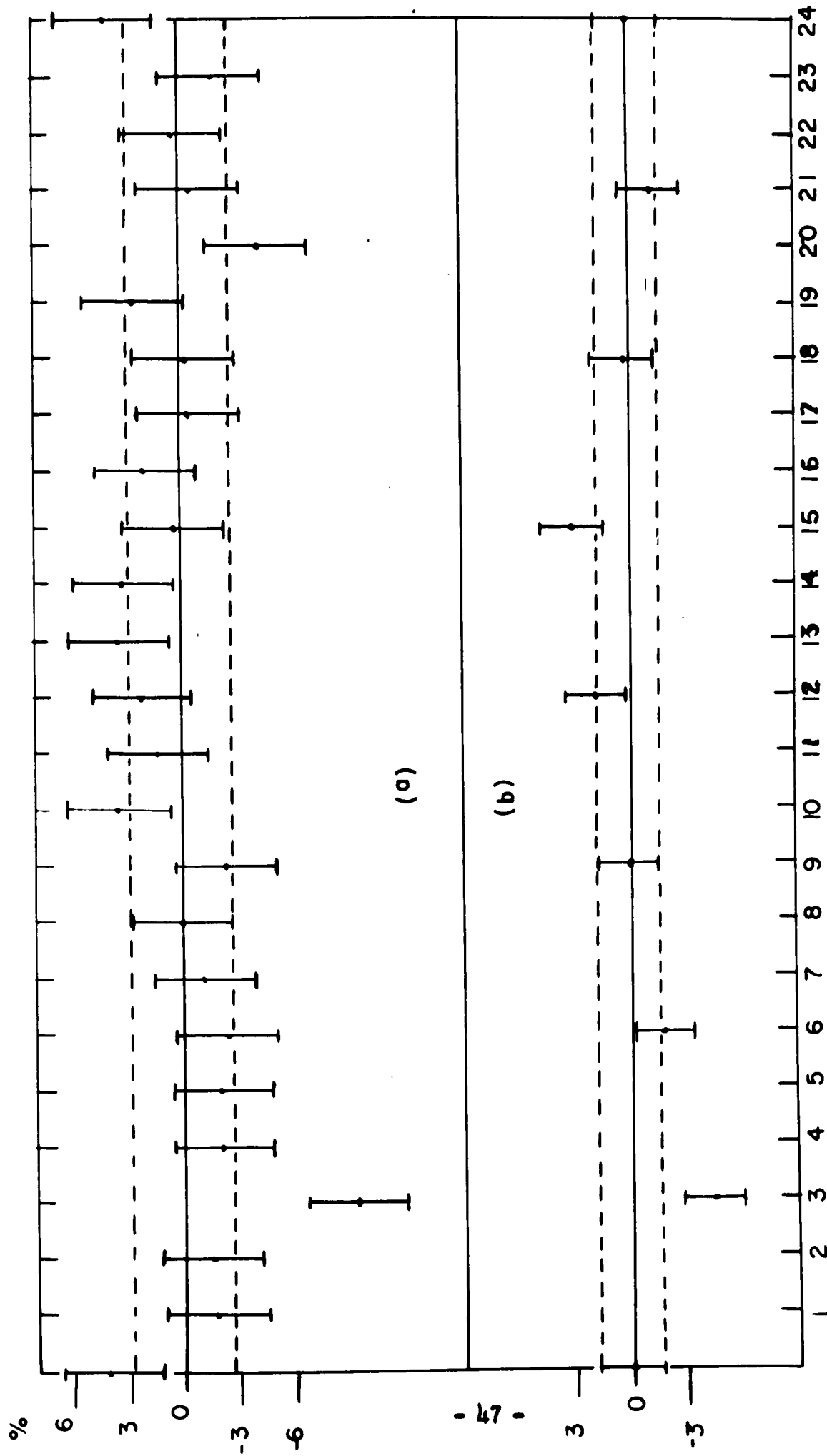


Fig. 12—% Deviation from mean for Calgary 3-6 folds VS LST for

(a) 1-hour intervals (b) 3-hour intervals.

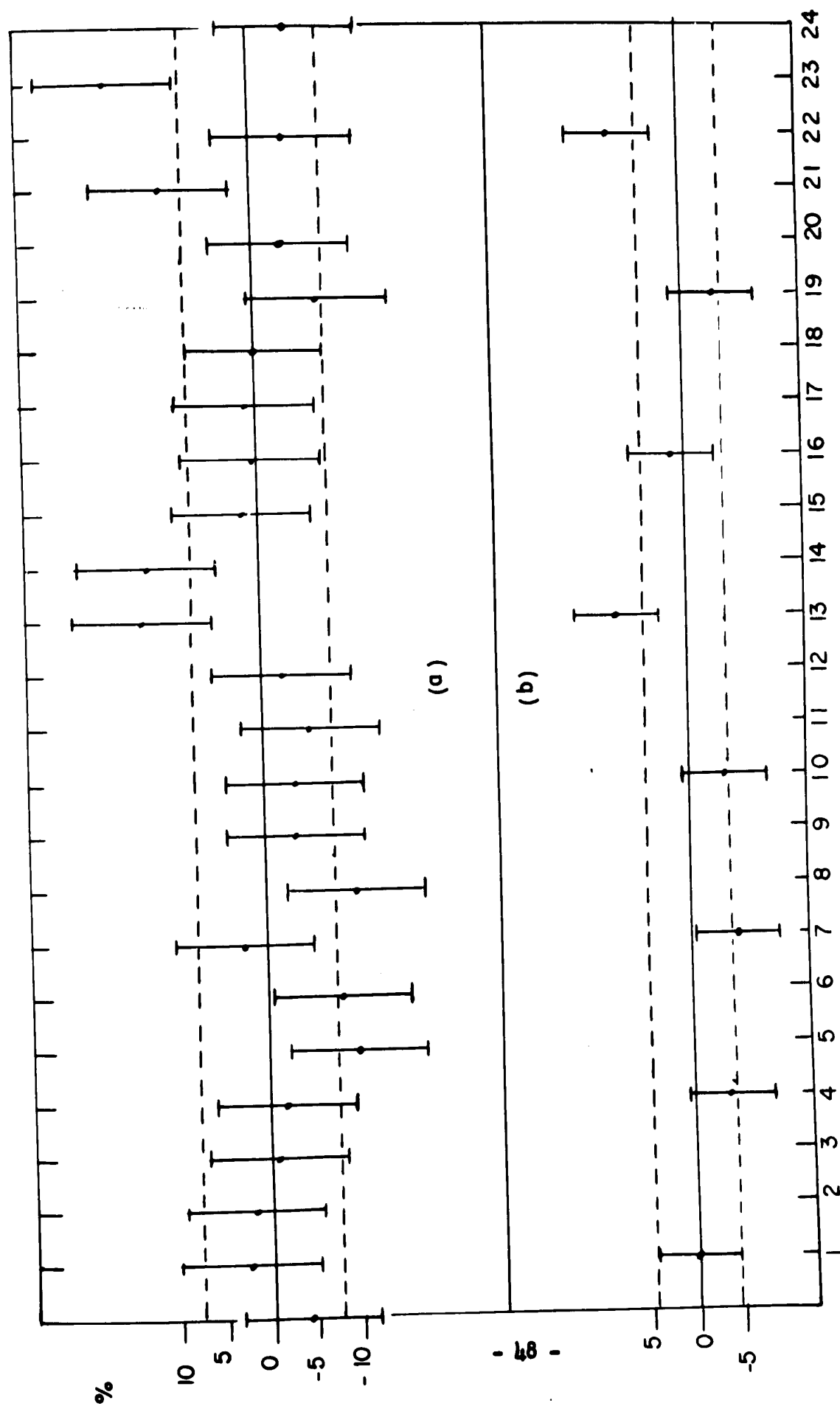


Fig. 13—%Deviation from mean for Calgary 7-12 folds VS LST for  
 (a) 1-hour intervals (b) 3-hour intervals.

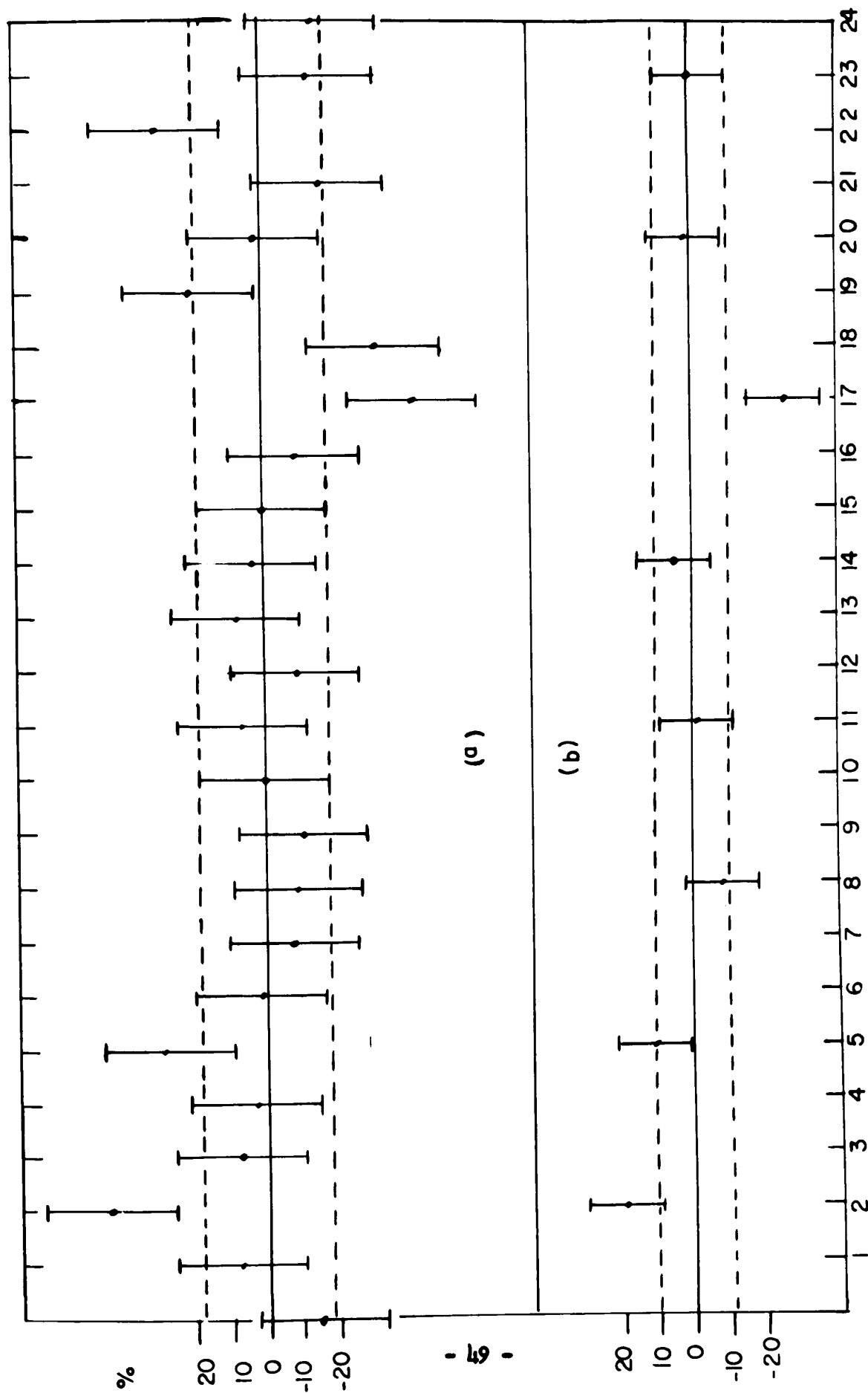


Fig. 14— %Deviation from mean for Calgary 13-18 folds VS LST for  
 (a) 1-hour intervals (b) 3-hour intervals.



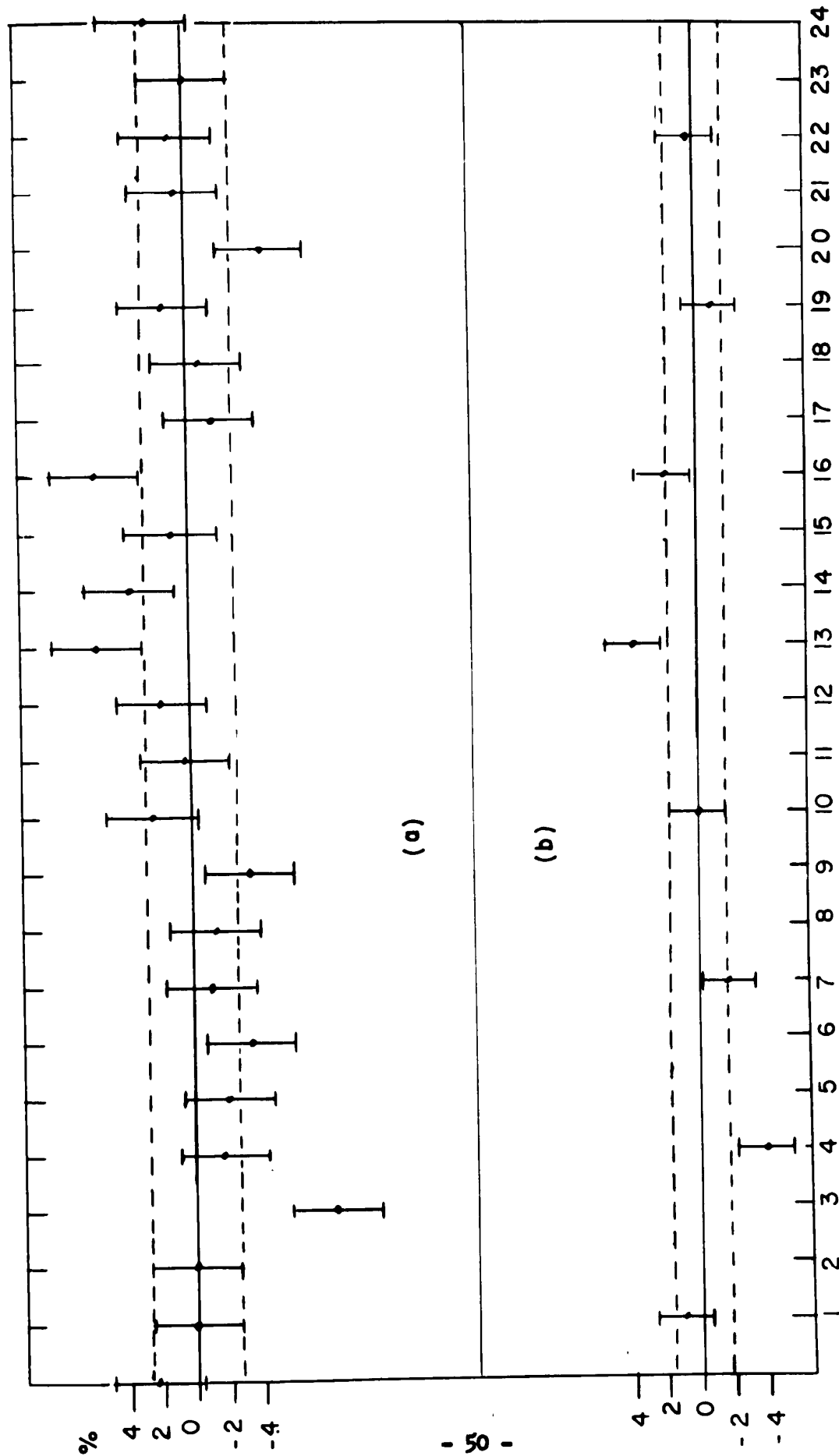


Fig. 15— % Deviation from total mean for Calgary VS LST for

(a) 1-hour intervals (b) 3-hour intervals.

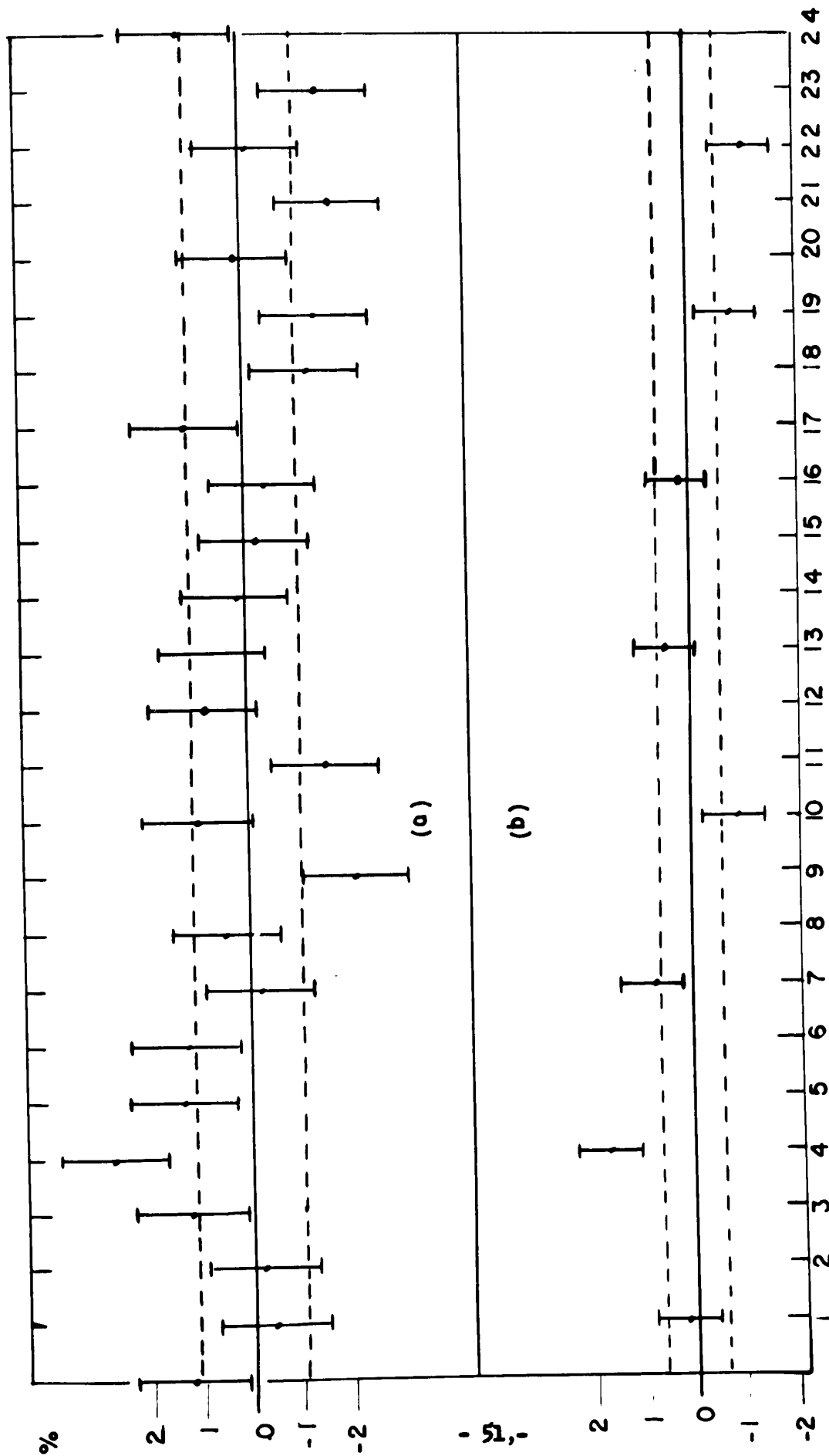


Fig. 16- % Deviation from mean for Banff 3-6 folds VS GMT  
for (a) 1-hour intervals (b) 3-hour intervals.

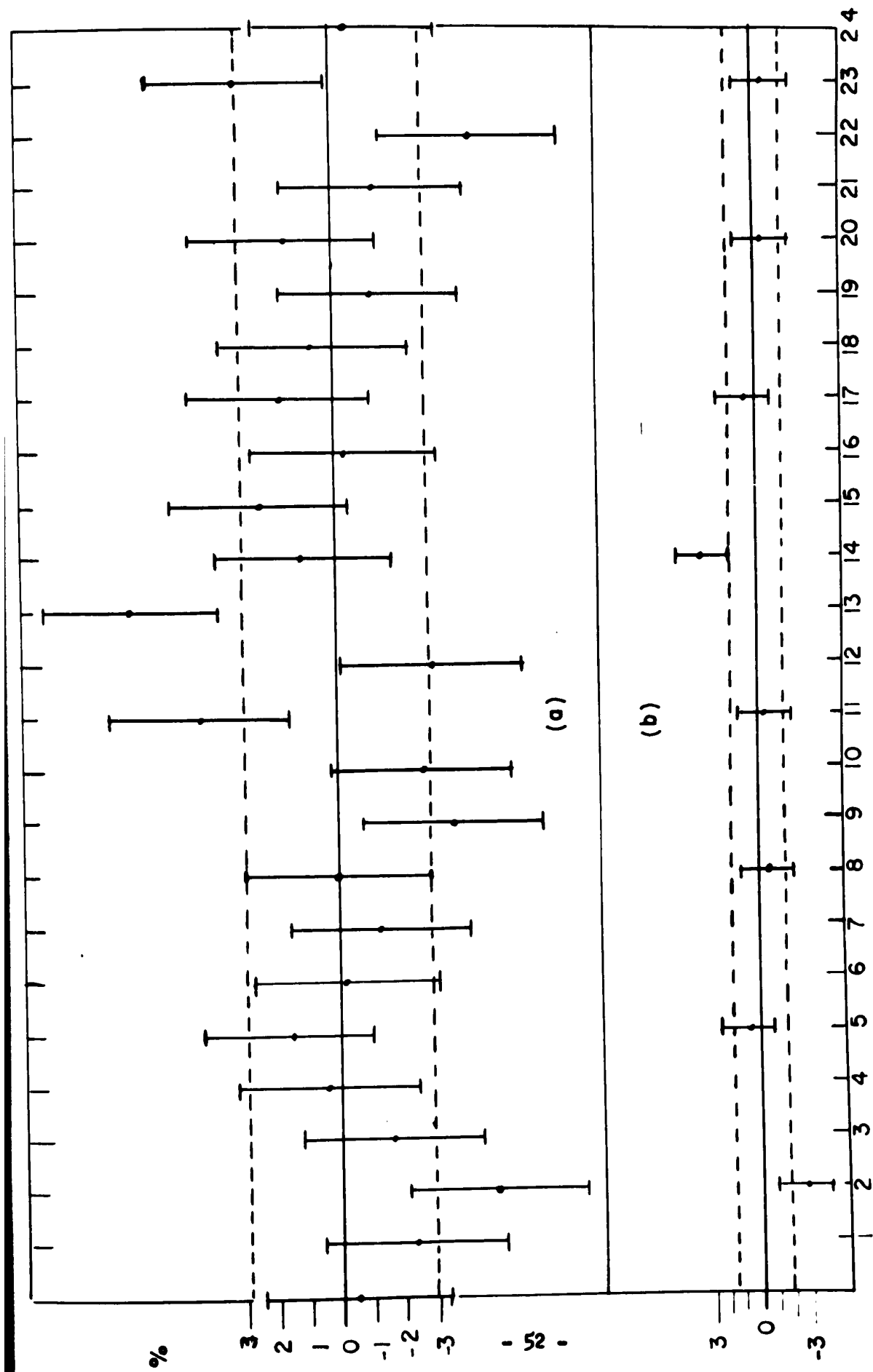


Fig. 17—% Deviation from mean for Banff 7-12 folds VS GMT for  
 (a) 1-hour intervals (b) 3-hour intervals.

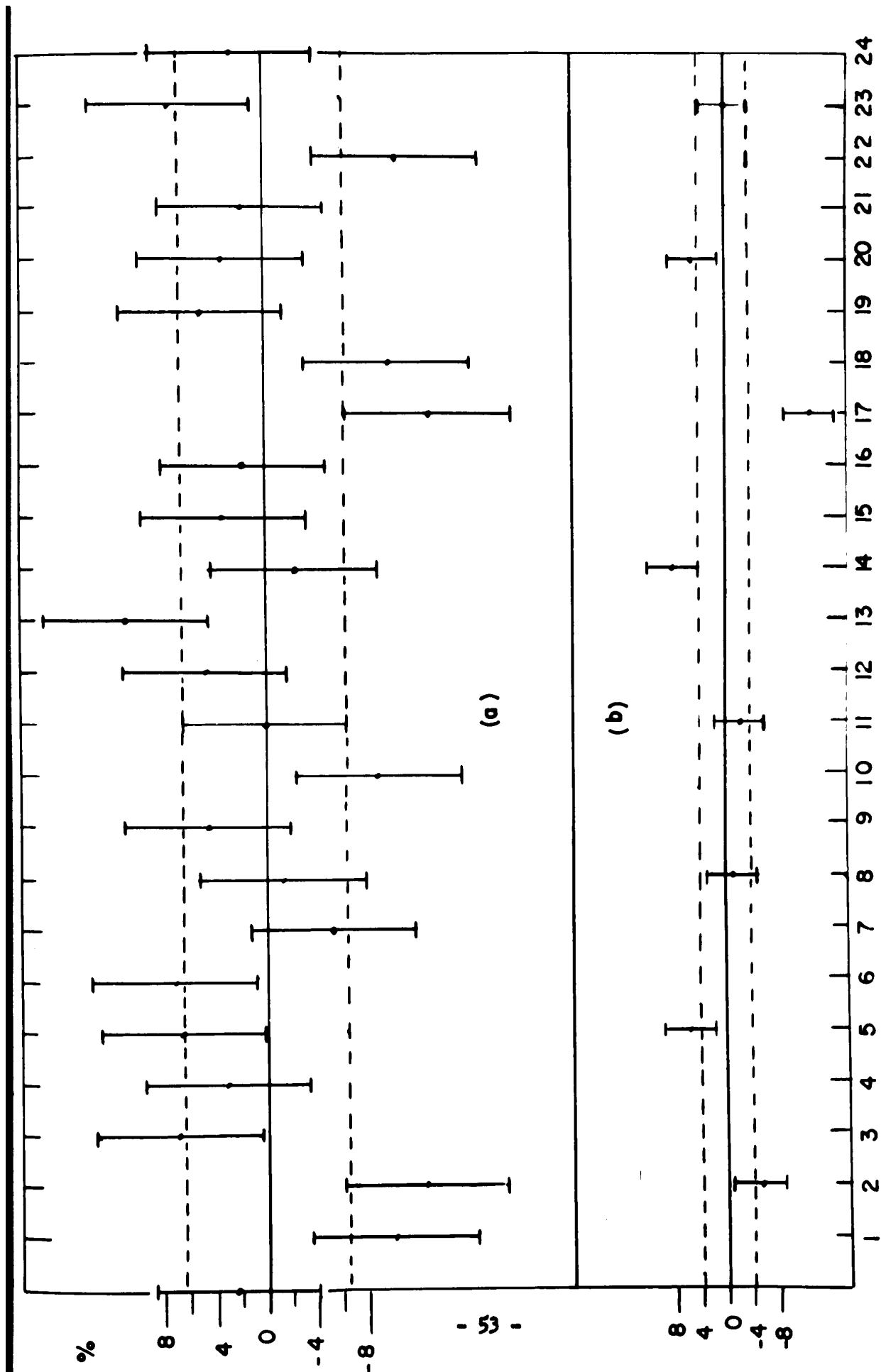


Fig. 18— % Deviation from mean for Banff 13-18 folds VS GMT for  
 (a) 1-hour intervals (b) 3-hour intervals.

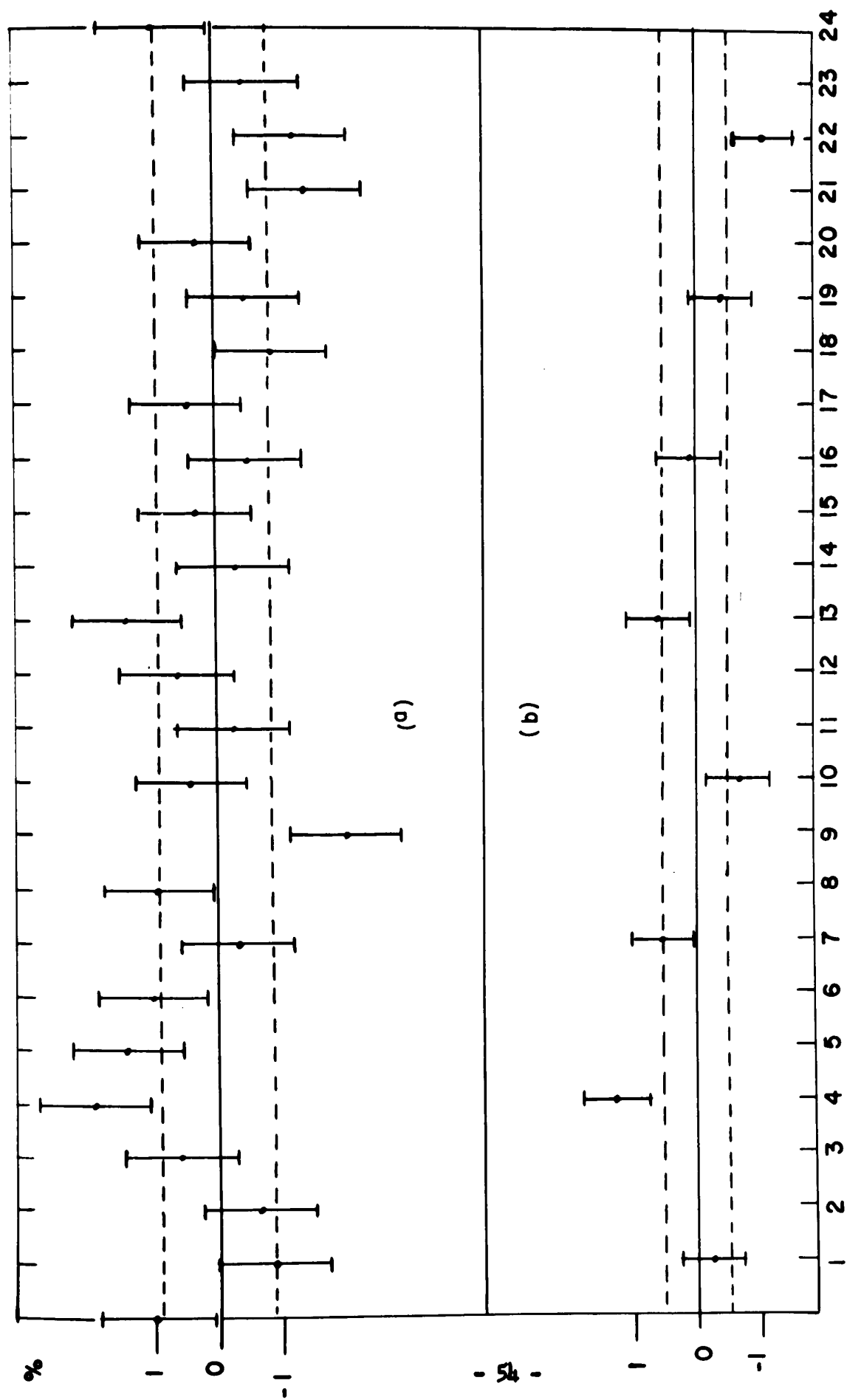


Fig. 19— % Deviation from total mean for Banff VS GMT for  
 (a) 1— hour intervals (b) 3—hour intervals.

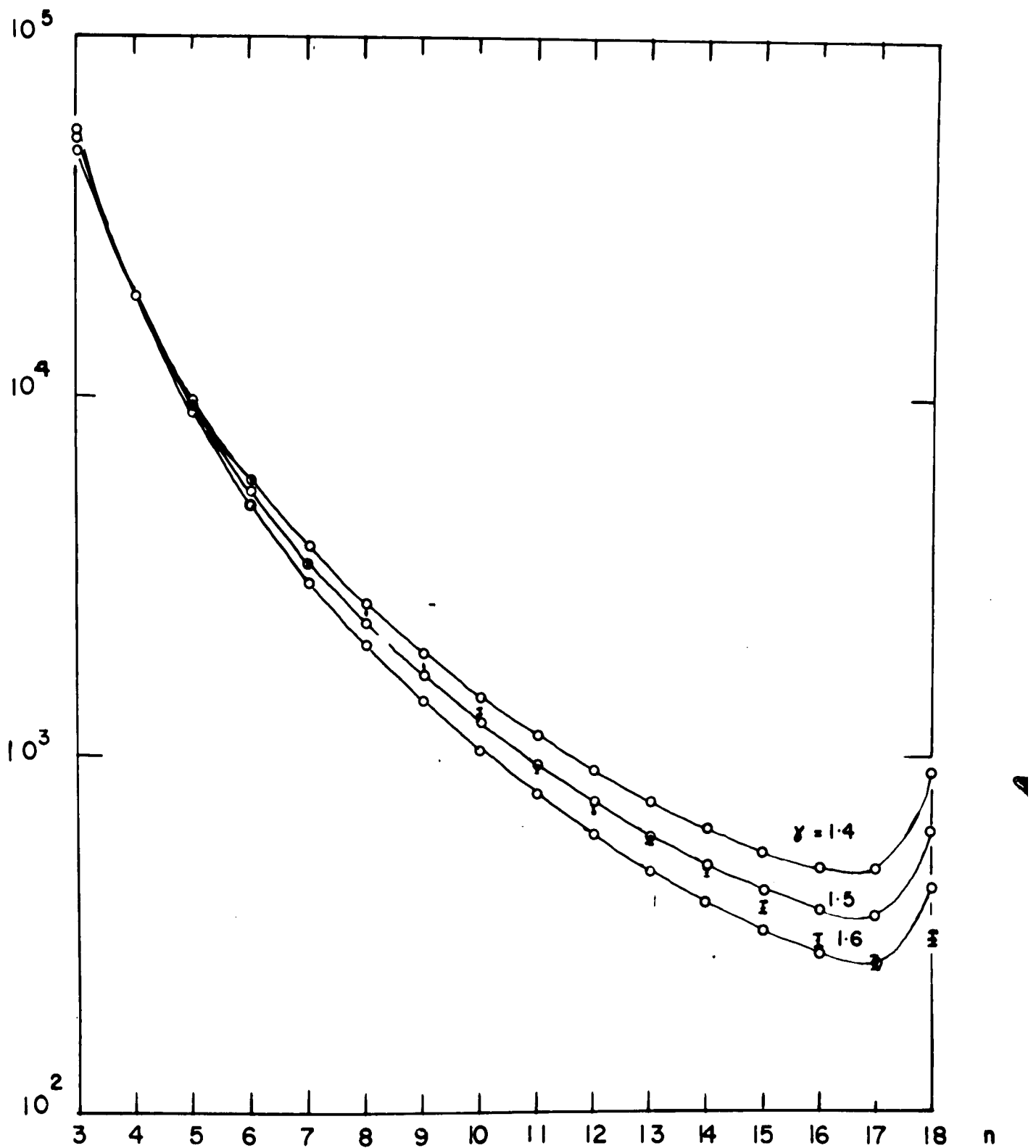


Fig. 20- Experimental number of showers  $N_s$  VS multiplicity  $n$  compared with predicted values with  $\gamma = 1.4, 1.5$  and  $1.6$ .

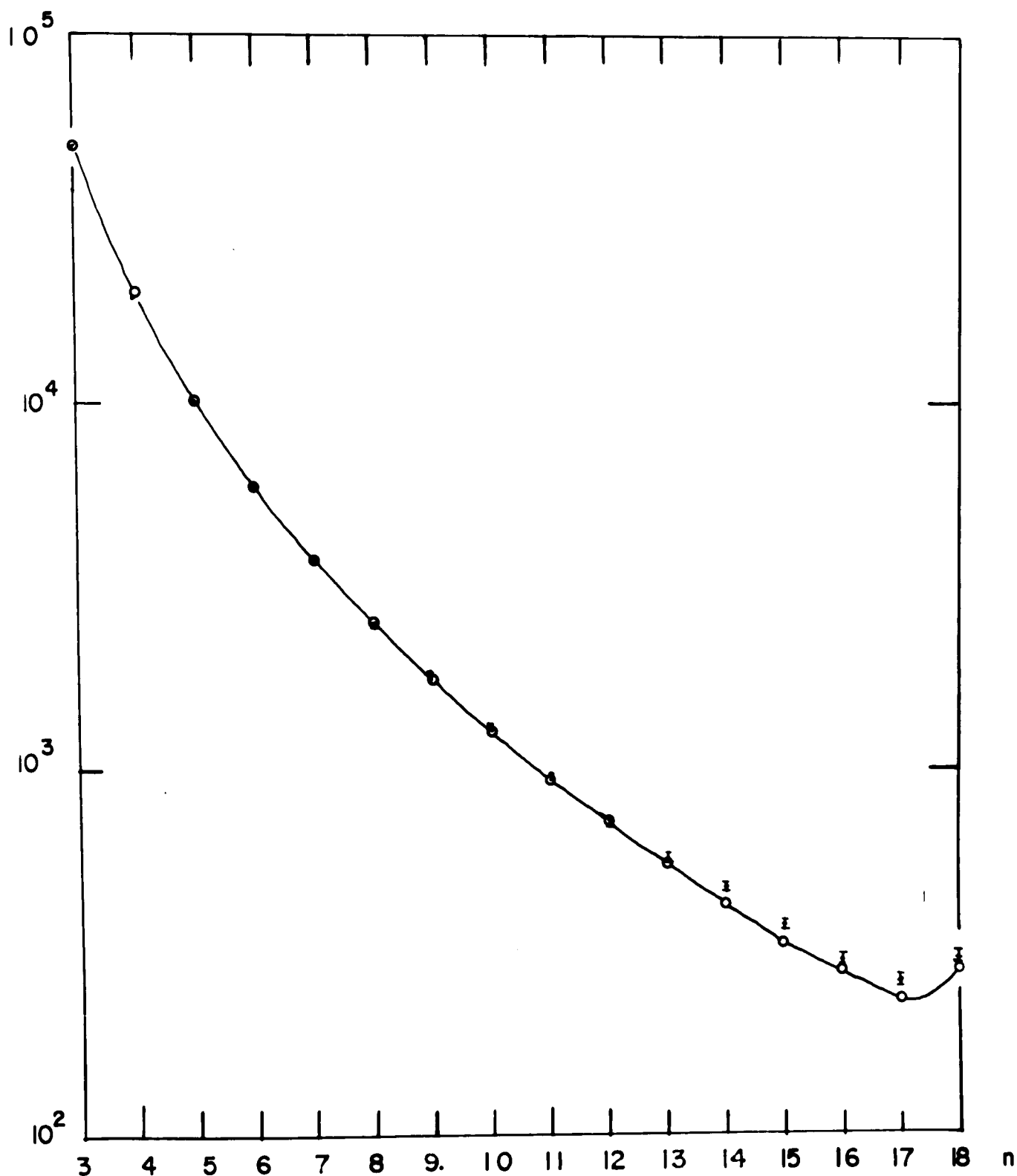


Fig. 21- Experimental number of showers  $N_s$  VS  
multiplicity  $n$  compared with predicted  
values using a variable  $\gamma$  from 1.4 - 2.0.

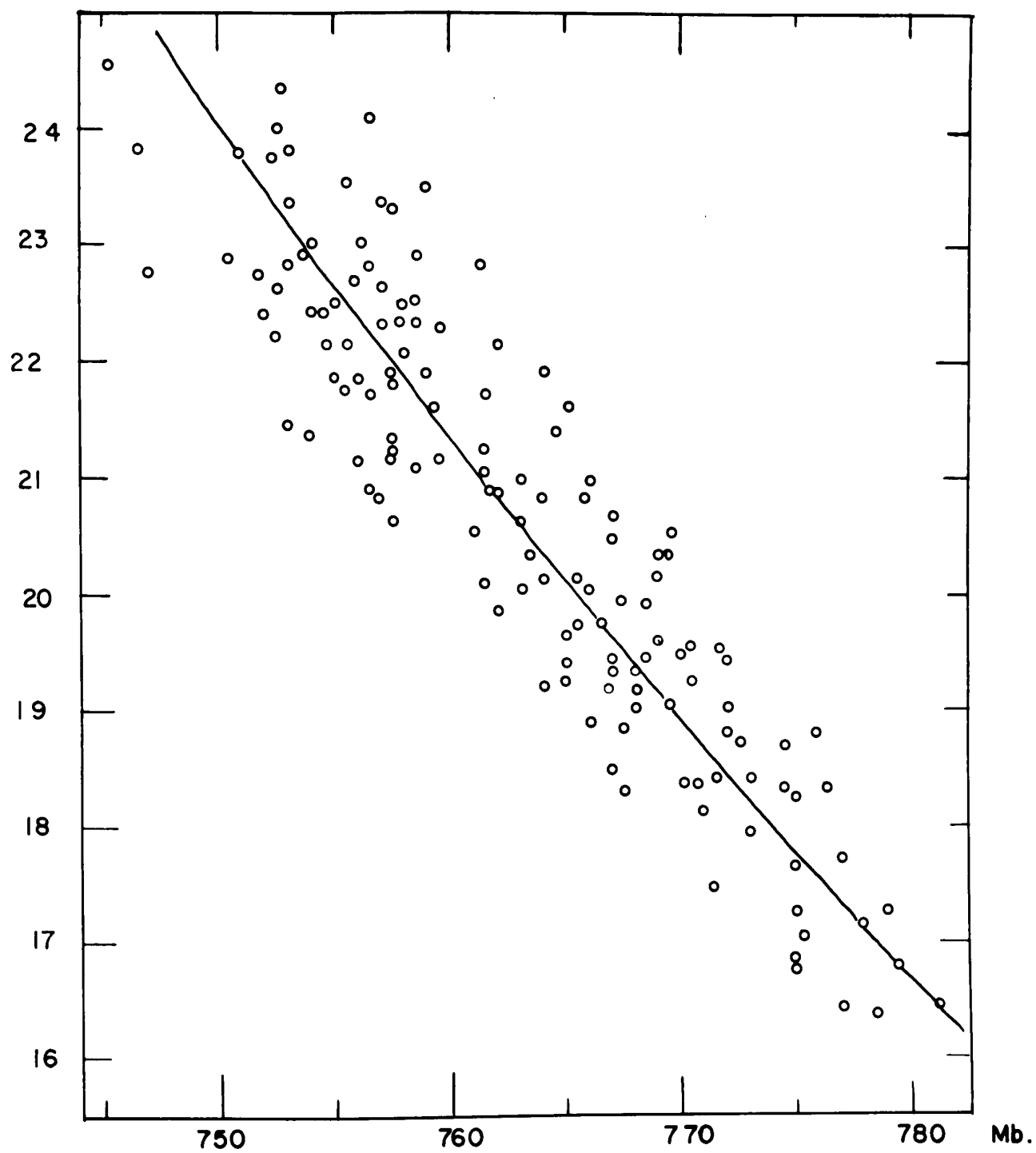


Fig. 22 — E.A.S. rate in counts per hour VS daily  
average pressure.



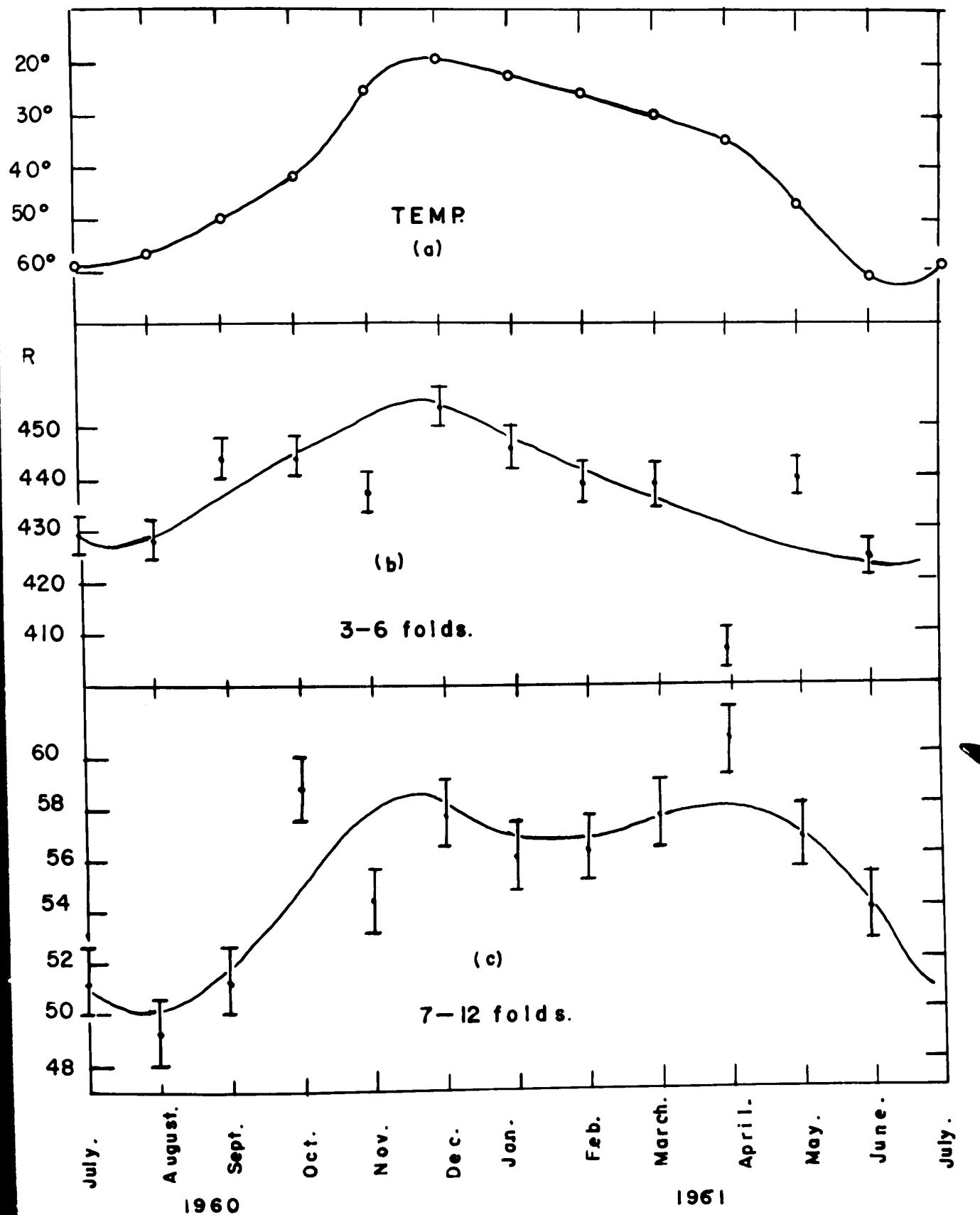


Fig. 23 (a) Banff monthly mean temperature VS month of year.  
 (b) 3-6 fold monthly mean rate VS month .  
 (c) 7-12 fold monthly mean rate VS month.

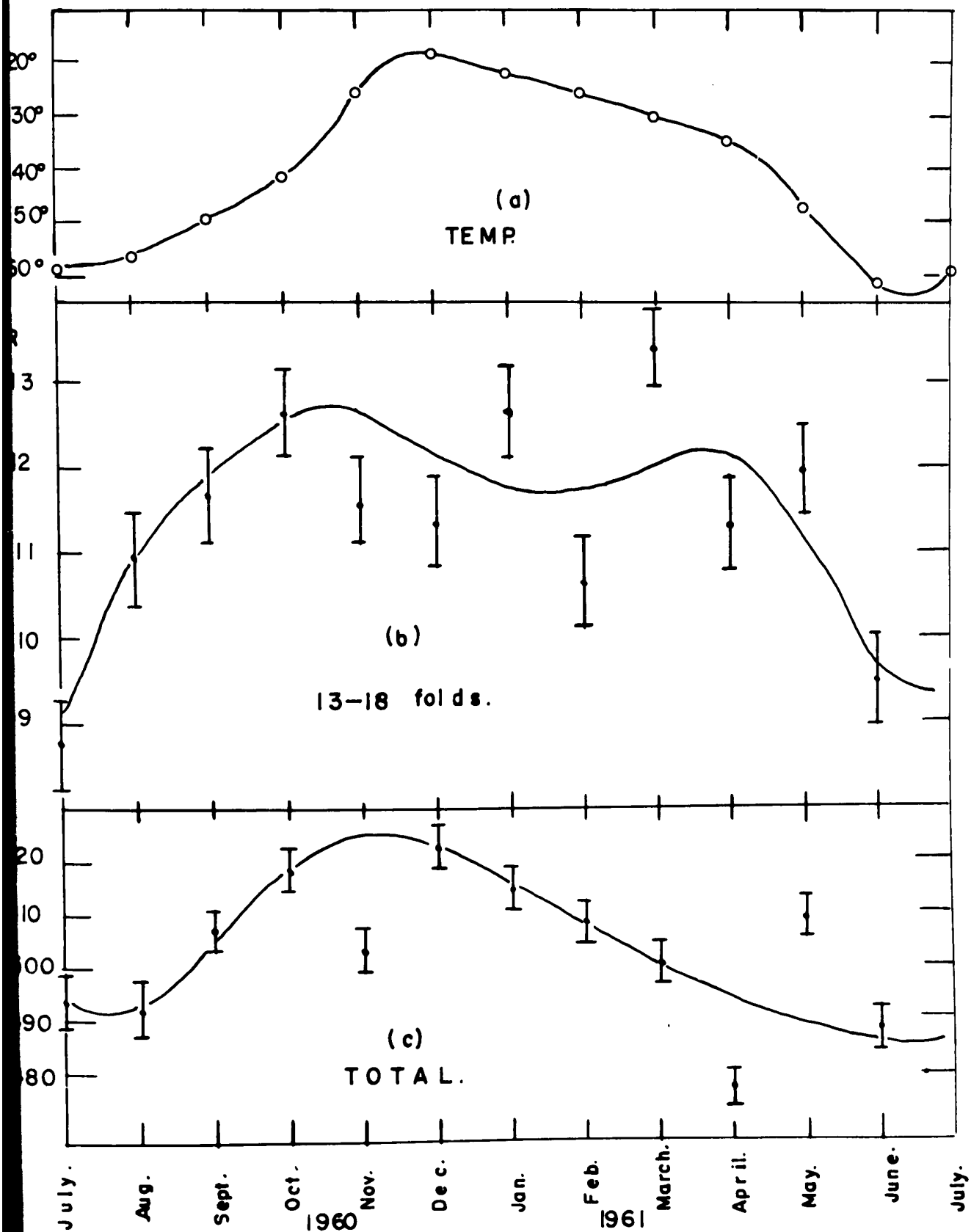


Fig. 24 (a) Banff monthly mean temperature VS month of year  
 (b) 13-18 fold monthly mean rate VS month.  
 (c) Total monthly mean rate - 59 VS month.

## Conclusion

(a) Time Variations When  $\chi^2$  tests were applied to the twenty four hourly results for Banff solar and sidereal time, and Calgary sidereal time, it was found in each case that the calculated sine wave through the experimental results gave a better fit than did a straight line; in each case, however, the amplitude of the sine wave was less than the corresponding statistical error. Since the sine wave was the best fit, and the statistical error was approximately the same for the sine wave as for the straight line, the amplitude of the sine wave was added to the statistical error and this sum was assumed as the maximum possible amplitude of the deviation from the mean in each case.

For the Banff solar data, the times corresponding to maximum counting rates for the three energy levels appear to have a random distribution i.e. 04.53 G.M.T., 12.40 G.M.T., and 10.11 G.M.T. The amplitudes of the maximum deviations become increasingly larger from 3-6 folds to 13-18 folds as would be expected due to the lessening of the statistical accuracy as the energy increases and the number decreases. For the total Banff solar counts the amplitude of the maximum deviation from the mean is 1.45% at 05.33 G.M.T. The probability of the data being best represented by a straight line is .14, and for a sine wave .22. These values are not small enough to justify saying that there is a variation in solar time, especially as the corresponding probabilities for the three components are all larger than those for the total. From Fig. 19 it can be seen that there is no obvious variation in the shower rate with solar time, and this result is consistent with previous results<sup>7</sup> in solar time from this experiment.

These results are not in agreement with those obtained by Mc Cusker et. al.<sup>9,10.</sup> who obtained much larger amplitudes using M-units as detectors.

The M-units however are sensitive to the core of the E.A.S. whereas the Banff apparatus detects any part of the shower. In an attempt to detect the variations observed by Mc Cusker, several M-units have been constructed and are at present operating satisfactorily in the cosmic ray laboratory in the penthouse of the Science Building at U.A.C.; the M-units have not been operating long enough to give good enough statistics to include in this report.

The Banff and Calgary sidereal data indicate no significant variation with local sidereal time; the times for the maximum deviations for the three components in each case have random distribution, except for the 3-6 fields which have approximately the same time for maximum deviation i.e. 13.37 L.S.T. for Banff and 13.47 L.S.T. for Calgary. The probabilities of the data representing straight lines however are .76 for Banff 3-6 fields and .10 for Calgary 3-6 fields; this latter value is still not small enough to indicate any variation with sidereal time. The low probability for the Calgary data is partly due to the fact that the Calgary data is only for 200 days compared with 545 days for the Banff data; for this reason the total Calgary data is only isotropic to 4.6% whereas the total Banff data is isotropic to 1.07%. The entire sidereal data is consistent with no significant variation in local sidereal time. These results agree with those obtained by most other workers, who have found either no variation, or only a very small variation of E.A.S. with local sidereal time, as can be seen from table 1.

(b) Density Spectrum

The experimental number of showers of each multiplicity has been obtained from two years data and normalised to a total of 100,000 events. They are tabulated in table 8 along with the predicted number of showers assuming a variable  $\gamma$  from 1.4 to 2.0. In fig. 20 the experimental number of showers is plotted against multiplicity and compared with the calculated number of showers for  $\gamma = 1.4, 1.5$  and  $1.6$ . It can be seen that up to 14-fold events, the experimental results indicate a value of  $\gamma$  of  $1.5 \pm 0.1$ , which is the same as that obtained by Dienne. Above 14-folds the data is consistent with an increasing value of  $\gamma$ . In fig. 21 the experimental number of showers is plotted against multiplicity and compared with the predicted values with  $\gamma$  varying from 1.4 to 2.0 as in table 8. The experimental results agree very well with the calculated values, confirming the prediction of a value of  $\gamma$  increasing with energy. These results agree very well with the results obtained by Dienne, giving a value of  $\gamma = 1.5 \pm 0.1$  for a density range 30 - 500 particles / m<sup>2</sup> with the value of  $\gamma$  increasing up to 1.9 for 18-fold events.

(c) Barometer Coefficient.

In Fig. 22 the daily E.A.S. rate in counts per hour is plotted against the daily average pressure; the best line that can be drawn through these points corresponds to a barometer coefficient of - 16.46% / cm. Hg. Recent work<sup>11</sup> by Cranshaw, Galbraith et. al. suggests that the barometer coefficient of showers increases with shower size from  $- 9.9 \pm 0.7$  to  $- 18.1 \pm 0.7$  % / cm. Hg for shower sizes varying from  $7 \cdot 10^3$  to  $2 \cdot 10^7$  particles. For the Banff apparatus the range of shower sizes is from  $10^5$  to  $10^7$  particles, and a

value of  $- 16.46 \% / \text{cm. Hg.}$  is in good agreement with these values.

(d) Temperature Coefficient

In Fig. 23 and Fig. 24 the mean daily rate for the month for 3-6, 7-12, 13-18 and total counts is plotted against the month of the year and compared with the monthly mean temperature. There is a good correlation between 3-6 field counting rate and monthly mean temperature, corresponding to a temperature coefficient of  $- 0.34 \% / ^\circ\text{C}$  which is in good agreement with the value of  $- 0.35 \% / ^\circ\text{C}$  obtained by Dienne<sup>7</sup> and that of  $- 0.38 \pm .11 \% / ^\circ\text{C}$  obtained by Hedson.<sup>12</sup> The correlation between 7-12 fields and 13-18 fields and monthly mean temperature is less good, although there is a similarity between the general forms of the two curves; the agreement was not considered good enough to obtain temperature coefficients for 7-12 and 13-18 fields, although it appears to indicate a temperature coefficient which increases with increasing shower energy.

## BIBLIOGRAPHY

1. Earl, J.A., 1961, Phys. Rev. Letters, 6, 125.
2. Bierman, L., 1953, Ann. Rev. Nuclear Sci., 2, 335.
3. Clark, G.W., Earl, J., Kraushaar, W.L., Linsley, J., Rossi, B., Scherb, F. and Scott, D.W., 1961, Phys. Rev. 122, 637, and Rossi, B., Proceedings of the Moscow Cosmic Ray Conference, 1960, International Union of Pure and Applied Physics, Vol. II, 18.
4. Davis, L., 1954, Phys. Rev., 96, 743.
5. Ginsburg, V.L., 1958, Progress in Cosmic Ray Physics Vol. IV, Chapter V, and 1961, Soviet Physics Uspekhi, 3, 504.
6. Peters, B., 1959, Nuove Cimento, 8, Suppl. 2.
7. Dienne, J.G., 1960, "Observations on Extensive Air Showers at Mountain Altitudes," Master Degree Thesis, Alberta.
8. Greisen, K., 1960, Ann. Rev. Nuclear Sci., 10, 71.
9. Mc Cusker, C.B.A. and Wilson, B.G., 1956, Nuove Cimento, 10, 188.
10. Mc Cusker, C.B.A., Page, D.E. and Reid, R.A., 1959, Phys. Rev., 113, 712.
11. Cranshaw, T.E., Galbraith, W., Porter, N.A., de Beer, J., and Hillas, M., 1958, Nuove Cimento, Supp. No. 2, 567.
12. Hedson, A.L., 1958, Quoted in Galbraith "Extensive Air Showers", Butterworths Scientific Publications, London, P. 133.

### General References

1. "Extensive Air Showers", W. Galbraith,  
Butterworths Scientific Publications, London, 1958.
2. "The Extensive Air Showers", K. Greisen,  
Progress in Cosmic Ray Physics, Vol III,  
North-Holland Publishing Company Amsterdam, 1956.
3. "The Origin of Cosmic Radiation", V.L. Ginzburg,  
Progress in Elementary Particle and Cosmic Ray  
Physics, Vol. IV, North-Holland Publishing Company  
Amsterdam, 1958.
4. "Cosmic Ray Showers", K. Greisen, Annual Review of  
Nuclear Science, Vol. 10, 1960.